Journal of Geotechnical and Geoenvironmental Engineering

Impact dynamics of boulder-enriched debris flow on a rigid barrier

--Manuscript Draft--

Manuscript Number:	GTENG-8770R1
Full Title:	Impact dynamics of boulder-enriched debris flow on a rigid barrier
Manuscript Region of Origin:	HONG KONG
Article Type:	Technical Paper
Manuscript Classifications:	13.01: Geohazards; 13.01.04: Landslides; 13.05.01.03: Retaining structures
Funding Information:	National Natural Science Foundation of China (51709052) — Clarence E. Choi Research Grants Council, University Grants Committee (AoE/E-603/18) — Charles W.W. Ng Research Grants Council, University Grants Committee (T22-603/15-N) — Charles W.W. Ng Research Grants Council, University Grants Committee (16212618) — Clarence E. Choi Research Grants Council, University Grants Committee (16209717) — Clarence E. Choi
Abstract:	Boulders entrained in debris flow induce high impact forces on a rigid barrier. In current design practice, the concentrated load from boulders is estimated using the Hertz equation with a load reduction factor (K_c). Separately, the distributed load from the debris is estimated using the hydrodynamic equation. The existing design practice is simply adding the estimated loads using the two equations. The interaction between debris flow and boulders during the impact process is neglected. In this study, physical tests were conducted using a newly-developed 28-m-long flume to shed light on the impact dynamics of debris flows with and without boulders on an instrumented rigid barrier. Contrary to existing design practice where the boulder and debris impact loads are added together, the debris provided a cushioning effect to attenuate the impact force of the boulders. This cushioning effect was governed by a reflection wave with a length scale L_R/d (where d is the boulder diameter), which serves as cushioning thickness upon impact. L_R/d from 0.4 to 2.0 can reduce the impact load by up to 80% compared to existing design practice (K_c = 0.1).
Corresponding Author:	Haiming Liu, Ph.D Hong Kong University of Science and Technology Hong Kong, HONG KONG
Corresponding Author E-Mail:	hliubc@connect.ust.hk
Order of Authors:	Charles W.W. Ng, PhD Haiming Liu, Ph.D Clarence E. Choi, PhD Julian S.H. Kwan, PhD W.K. Pun
Additional Information:	
Question	**Response**
Authors are required to attain permission to re-use content, figures, tables, charts, maps, and photographs for which the authors do not hold copyright. Figures	No

created by the authors but previously published under copyright elsewhere may require permission. For more information see http://ascelibrary.org/doi/abs/10.1061/9780784479018.ch03. All permissions must be uploaded as a permission file in PDF format. Are there any required permissions that have not yet been secured? If yes, please explain in the comment box.	
ASCE does not review manuscripts that are being considered elsewhere to include other ASCE Journals and all conference proceedings. Is the article or parts of it being considered for any other publication? If your answer is yes, please explain in the comments box below.	No
Each submission to ASCE must stand on its own and represent significant new information, which may include disproving the work of others. While it is acceptable to build upon one's own work or replicate other's work, it is not appropriate to fragment the research to maximize the number of manuscripts or to submit papers that represent very small incremental changes. ASCE may use tools such as CrossCheck, Duplicate Submission Checks, and Google Scholar to verify that submissions are novel. Does the manuscript constitute incremental work (i.e. restating raw data, models, or conclusions from a previously published study)?	No
Authors are expected to present their papers within the page limitations described in <u><i>Publishing in ASCE Journals: A Guide for Authors</u></i>. Technical papers and Case Studies must not exceed 30 double-spaced manuscript pages, including all figures and tables. Technical notes must not exceed 7 double-spaced manuscript pages. Papers that exceed the limits must be justified. Grossly over-length papers may be returned without review. Does this paper exceed the ASCE length limitations? If yes, please provide justification in the comments box below.	No
All authors listed on the manuscript must	No

have contributed to the study and must approve the current version of the manuscript. Are there any authors on the paper that do not meet these criteria? If the answer is yes, please explain in the comments.	
Was this paper previously declined or withdrawn from this or another ASCE journal? If so, please provide the previous manuscript number and explain what you have changed in this current version in the comments box below. You may upload a separate response to reviewers if your comments are extensive.	No
Companion manuscripts are discouraged as all papers published must be able to stand on their own. Justification must be provided to the editor if an author feels as though the work must be presented in two parts and published simultaneously. There is no guarantee that companions will be reviewed by the same reviewers, which complicates the review process, increases the risk for rejection and potentially lengthens the review time. If this is a companion paper, please indicate the part number and provide the title, authors and manuscript number (if available) for the companion papers along with your detailed justification for the editor in the comments box below. If there is no justification provided, or if there is insufficient justification, the papers will be returned without review.	
If this manuscript is intended as part of a Special Issue or Collection, please provide the Special Collection title and name of the guest editor in the comments box below.	
Recognizing that science and engineering are best served when data aremade available during the review and discussion of manuscripts andjournal articles, and to allow others to replicate and build on workpublished in ASCE journals, all reasonable requests by reviewers formaterials, data, and associated protocols must be fulfilled. If you are restricted from sharing your data and materials, please explain below.	

Papers published in ASCE Journals must make a contribution to the core body of knowledge and to the advancement of the field. Authors must consider how their new knowledge and/or innovations add value to the state of the art and/or state of the practice. Please outline the specific contributions of this research in the comments box.	1. The impact dynamics of flow-like landslide (debris flow) with and without boulders on a rigid barrier are examined by carrying out a series of large-scale flume tests. 2. Contrary to existing design practice where the boulder and debris impact loads are added together, experiment results show that the debris provided a cushioning effect to attenuate the impact force of the boulders. This cushioning effect was governed by a reflection wave, which serves as cushioning layer upon impact. 3. A new equation has been proposed and evaluated to estimate the load reduction factor with consideration of debris cushioning effects. This equation can serve as a basis of impact load optimization for designing landslide barriers.
The flat fee for including color figures in print is $800, regardless of the number of color figures. There is no fee for online only color figures. If you decide to not print figures in color, please ensure that the color figures will also make sense when printed in black-and-white, and remove any reference to color in the text. Only one file is accepted for each figure. Do you intend to pay to include color figures in print? If yes, please indicate which figures in the comments box.	No
Is this article or parts of it already published in print or online in any language? ASCE does not review content already published (see next questions for conference papers and posted theses/dissertations). If your answer is yes, please explain in the comments box below.	No
Has this paper or parts of it been published as a conference proceeding? A conference proceeding may be reviewed for publication only if it has been significantly revised and contains 50% new content. Any content overlap should be reworded and/or properly referenced. If your answer is yes, please explain in the comments box below and be prepared to provide the conference paper.	No
ASCE allows submissions of papers that are based on theses and dissertations so long as the paper has been modified to fit the journal page limits, format, and tailored for the audience. ASCE will consider such papers even if the thesis or dissertation has been posted online provided that the degree-granting institution requires that the thesis or	No

dissertation be posted. Is this paper a derivative of a thesis or dissertation posted or about to be posted on the Internet? If yes, please provide the URL or DOI permalink in the comment box below.	
When submitting a new and revised manuscript, authors are asked to include a Data Availability Statement containing one or more of the following statements, with specific items listed as appropriate. Please select any of the statements below that apply to your manuscript. Also, please include the selected statements in a separate "Data Availability Statement" section in your manuscript, directly before the acknowledgements or references. The statement(s) listed in your manuscript should match those you select in your response to this question.	c. Some or all data, models, or code that support the findings of this study are available from the corresponding author upon reasonable request.
If there is anything else you wish to communicate to the editor of the journal, please do so in this box.	
COPYRIGHT TRANSFER AGREEMENT **I. Authorship Responsibility** To protect the integrity of authorship, only people who have significantly contributed to the research or project and manuscript preparation shall be listed as coauthors. The corresponding author attests to the fact that anyone named as a coauthor has seen the final version of the manuscript and has agreed to its submission for publication. Deceased persons who meet the criteria for coauthorship shall be included, with a footnote reporting date of death. No fictitious name shall be given as an author or coauthor. An author who submits a manuscript for publication accepts responsibility for having properly included all, and only, qualified coauthors.	None of the exceptions listed above apply.

II. Originality of Content

ASCE respects the copyright ownership of other publishers. ASCE requires authors to obtain permission from the copyright holder to reproduce any material that (1) they did not create themselves and/or (2) has been previously published, to include the authors' own work for which copyright was transferred to an entity other than ASCE. For any figures, tables, or text blocks exceeding 100 words from a journal article or 500 words from a book, written permission from the copyright holder must be obtained and supplied with the submission. Each author has a responsibility to identify materials that require permission by including a citation in the figure or table caption or in extracted text.

More information can be found in the guide "Publishing in ASCE Journals: Manuscript Submission and Revision Requirements" (http://ascelibrary.org/doi/pdf/10.1061/9780784479018.ch05). Regardless of acceptance, no manuscript or part of a manuscript will be published by ASCE without proper verification of all necessary permissions to re-use. ASCE accepts no responsibility for verifying permissions provided by the author. Any breach of copyright will result in retraction of the published manuscript.

III. Copyright Transfer

ASCE requires that authors or their agents assign copyright to ASCE for all original content published by ASCE. The author(s) warrant(s) that the above-cited manuscript is the original work of the author(s) and has never been published in its present form.

The undersigned, with the consent of all authors, hereby transfers, to the extent that there is copyright to be transferred, the exclusive copyright interest in the above-cited manuscript (subsequently called the “work”) in this and all subsequent editions of the work (to include closures and errata), and in derivatives, translations, or ancillaries, in English and in foreign translations, in all formats and media of expression now known or later developed, including electronic, to the American Society of Civil Engineers subject to the following:

• The undersigned author and all coauthors retain the right to revise, adapt, prepare derivative works, present orally, or distribute the work, provided that all such use is for the personal noncommercial benefit of the author(s) and is consistent with any prior contractual agreement between the undersigned and/or coauthors and their employer(s).

• No proprietary right other than copyright is claimed by ASCE.

• This agreement will be rendered null and void if (1) the manuscript is not accepted for publication by ASCE, (2) is withdrawn by the author prior to publication (online or in print), (3) ASCE Open Access is purchased by the author.

• Authors may post a PDF of the ASCE-published version of their work on their employers’ ***Intranet*** with password protection. The following statement must appear with the work: “This material may be downloaded for personal use only. Any other use requires prior permission of the American Society of Civil Engineers.”

• Authors may deposit the ***final draft*** of their work in an institutional repository or in their funding body's designated archive upon publication in an ASCE Journal, provided the draft contains a link to the published version at ascelibrary.org, and may request public access 12 months after publication. "Final draft" means the version submitted to ASCE after peer review and prior to copyediting or other ASCE production activities; it does not include the copyedited version, the page proof, a PDF, or full-text HTML of the published version.

• Authors may post the ***final draft*** of their work on open, unrestricted Internet sites 12 months after publication in an ASCE Journal, provided the draft contains a link to the published version at ascelibrary.org.

Exceptions to the Copyright Transfer policy exist in the following circumstances. Select the appropriate option below to indicate whether you are claiming an exception:

• **U.S. GOVERNMENT EMPLOYEES**: Work prepared by U.S. Government employees in their official capacities is not subject to copyright in the United States. Such authors must place their work in the public domain, meaning that it can be freely copied, republished, or redistributed. In order for the work to be placed in the public domain, ALL AUTHORS must be official U.S. Government employees. If at least one author is not a U.S. Government employee, copyright must be transferred to ASCE by that author.

• **CROWN GOVERNMENT COPYRIGHT**: Whereby a work is prepared by officers of the Crown Government in their official capacities, the Crown Government reserves its own copyright under national law. If ALL AUTHORS on the manuscript

are Crown Government employees, copyright cannot be transferred to ASCE; however, ASCE is given the following nonexclusive rights: (1) to use, print, and/or publish in any language and any format, print and electronic, the above-mentioned work or any part thereof, provided that the name of the author and the Crown Government affiliation is clearly indicated; (2) to grant the same rights to others to print or publish the work; and (3) to collect royalty fees. ALL AUTHORS must be official Crown Government employees in order to claim this exemption in its entirety. If at least one author is not a Crown Government employee, copyright must be transferred to ASCE by that author. • **WORK-FOR-HIRE**: Privately employed authors who have prepared works in their official capacity as employees must also transfer copyright to ASCE; however, their employer retains the rights to revise, adapt, prepare derivative works, publish, reprint, reproduce, and distribute the work provided that such use is for the promotion of its business enterprise and does not imply the endorsement of ASCE. In this instance, an authorized agent from the authors' employer must sign the form below. • **U.S. GOVERNMENT CONTRACTORS**: Work prepared by authors under a contract for the U.S. Government (e.g., U.S. Government labs) may or may not be subject to copyright transfer. Authors must refer to their contractor agreement. For works that qualify as U.S. Government works by a contractor, ASCE acknowledges that the U.S. Government retains a nonexclusive, paid-up, irrevocable, worldwide license to publish or reproduce this work for U.S. Government purposes only. This policy DOES NOT apply to work created with U.S. Government grants.	
Please type your name below to complete the copyright transfer agreement. This will serve as your digital signature.	Haiming LIU

I, the corresponding author, confirm that the authors listed on the manuscript are aware of their authorship status and qualify to be authors on the manuscript according to the guidelines above.

I, the corresponding author, confirm that the content, figures, drawings, charts, photographs, and tables in the submitted work are either original work created by the authors listed on the manuscript or work for which permission to re- use has been obtained from the creator.

I, the corresponding author, acting with consent of all authors listed on the manuscript, hereby transfer copyright or claim exemption to transfer copyright of the work as indicated above to the American Society of Civil Engineers.
as follow-up to "**COPYRIGHT TRANSFER AGREEMENT**

I. Authorship Responsibility

To protect the integrity of authorship, only people who have significantly contributed to the research or project and manuscript preparation shall be listed as coauthors. The corresponding author attests to the fact that anyone named as a coauthor has seen the final version of the manuscript and has agreed to its submission for publication. Deceased persons who meet the criteria for coauthorship shall be included, with a footnote reporting date of death. No fictitious name shall be given as an author or coauthor. An author who submits a manuscript for publication accepts responsibility for having properly included all, and only, qualified coauthors.

II. Originality of Content

ASCE respects the copyright ownership of other publishers. ASCE requires authors to obtain permission from the copyright holder to reproduce any material that (1) they did not create themselves and/or (2) has been previously published, to include the authors' own work for which copyright was transferred to an entity other than ASCE. For any figures, tables, or text blocks exceeding 100 words from a journal article or 500 words from a book, written permission from the copyright holder must be obtained and supplied with the submission. Each author has a responsibility to identify materials that require permission by including a citation in the figure or table caption or in extracted text.

More information can be found in the guide "Publishing in ASCE Journals: Manuscript Submission and Revision Requirements" (http://ascelibrary.org/doi/pdf/10.1061/9780784479018.ch05). Regardless of acceptance, no manuscript or part of a manuscript will be published by ASCE without proper verification of all necessary permissions to re-use. ASCE accepts no responsibility for verifying permissions provided by the author. Any breach of copyright will result in retraction of the published manuscript.

III. Copyright Transfer

ASCE requires that authors or their agents assign copyright to ASCE for all original content published by ASCE. The author(s) warrant(s) that the above-cited manuscript is the original work of the author(s) and has never been published in its present form.

The undersigned, with the consent of all authors, hereby transfers, to the extent that there is copyright to be transferred, the exclusive copyright interest in the above-cited manuscript (subsequently called the “work”) in this and all subsequent editions of the work (to include closures and errata), and in derivatives, translations, or ancillaries, in English and in foreign translations, in all formats and media of expression now known or later developed, including electronic, to the American Society of Civil Engineers subject to the following:

• The undersigned author and all coauthors retain the right to revise, adapt, prepare derivative works, present orally, or distribute the work, provided that all such use is for the personal noncommercial benefit of the author(s) and is consistent with any prior contractual agreement between the undersigned and/or coauthors and their employer(s).

• No proprietary right other than copyright is claimed by ASCE.

• This agreement will be rendered null and void if (1) the manuscript is not accepted for publication by ASCE, (2) is withdrawn by the author prior to publication (online or in print), (3) ASCE Open Access is purchased by the author.

• Authors may post a PDF of the ASCE-published version of their work on their employers’ ***Intranet*** with password protection. The following statement must appear with the work: “This material may be downloaded for personal use only. Any other use requires prior permission of the American Society of Civil Engineers.”

• Authors may deposit the ***final draft*** of their work in an institutional repository or in their funding body's designated archive upon publication in an ASCE Journal, provided the draft contains a link to the published version at ascelibrary.org, and may request public access 12 months after publication. "Final draft" means the version submitted to ASCE after peer review and prior to copyediting or other ASCE production activities; it does not include the copyedited version, the page proof, a PDF, or full-text HTML of the published version.

• Authors may post the ***final draft*** of their work on open, unrestricted Internet sites 12 months after publication in an ASCE Journal, provided the draft contains a link to the published version at ascelibrary.org.

Exceptions to the Copyright Transfer policy exist in the following circumstances. Select the appropriate option below to indicate whether you are claiming an exception:

• **U.S. GOVERNMENT EMPLOYEES**: Work prepared by U.S. Government employees in their official capacities is not subject to copyright in the United States. Such authors must place their work in the public domain, meaning that it can be freely copied, republished, or redistributed. In order for the work to be placed in the public domain, ALL AUTHORS must be official U.S. Government employees. If at least one author is not a U.S. Government employee, copyright must be transferred to ASCE by that author.

• **CROWN GOVERNMENT COPYRIGHT**: Whereby a work is prepared by officers of the Crown Government in their official capacities, the Crown Government

reserves its own copyright under national law. If ALL AUTHORS on the manuscript are Crown Government employees, copyright cannot be transferred to ASCE; however, ASCE is given the following nonexclusive rights: (1) to use, print, and/or publish in any language and any format, print and electronic, the above-mentioned work or any part thereof, provided that the name of the author and the Crown Government affiliation is clearly indicated; (2) to grant the same rights to others to print or publish the work; and (3) to collect royalty fees. ALL AUTHORS must be official Crown Government employees in order to claim this exemption in its entirety. If at least one author is not a Crown Government employee, copyright must be transferred to ASCE by that author. • **WORK-FOR-HIRE**: Privately employed authors who have prepared works in their official capacity as employees must also transfer copyright to ASCE; however, their employer retains the rights to revise, adapt, prepare derivative works, publish, reprint, reproduce, and distribute the work provided that such use is for the promotion of its business enterprise and does not imply the endorsement of ASCE. In this instance, an authorized agent from the authors' employer must sign the form below. • **U.S. GOVERNMENT CONTRACTORS**: Work prepared by authors under a contract for the U.S. Government (e.g., U.S. Government labs) may or may not be subject to copyright transfer. Authors must refer to their contractor agreement. For works that qualify as U.S. Government works by a contractor, ASCE acknowledges that the U.S. Government retains a nonexclusive, paid-up, irrevocable, worldwide license to publish or reproduce this work for U.S. Government purposes only. This policy DOES NOT apply to work created with U.S. Government grants."	

Manuscript ID: GTENG-8770R1 **9th July 2020**

Robb Eric S. Moss
Editor
ASCE Journal of Geotechnical and Geonvironmental Engineering

Dear Professor Moss,

Impact dynamics of boulder-enriched debris flow on a rigid barrier

By Charles W.W. Ng, Haiming Liu*, Clarence E. Choi, Julian S.H. Kwan and W.K. Pun

Thank you for your email dated 3rd June 2020 informing us that our manuscript has been requested for a revision based on the evaluations from the reviewers. We have now addressed all the comments from the reviewers on a point-by-point basis. The revised documents are as follows:

1. A copy of revised manuscript
2. A copy of our detailed responses to the comments from reviewers

Should you have any query, please do not hesitate to contact me at hliubc@connect.ust.hk. I look forward to hearing from you in due course.

Yours Sincerely,

Haiming Liu

Impact dynamics of boulder-enriched debris flow on a rigid barrier

Charles W.W. Ng[1], F.ASCE; Haiming Liu[2*]; Clarence E. Choi[3] ;
Julian S.H. Kwan[4]; W. K. Pun[5]

[1] Chair Professor, Department of Civil and Environmental Engineering, The Hong Kong University of Science and Technology, Hong Kong SAR, China

[2] Postdoctoral Fellow, Department of Civil and Environmental Engineering, The Hong Kong University of Science and Technology, Hong Kong SAR, China

[3] Assistant Professor, Department of Civil Engineering, The University of Hong Kong, Hong Kong SAR, China; The University of Hong Kong Shenzhen Institute of Research and Innovation, Nanshan, Shenzhen, China

[4] Chief Geotechnical Engineer, Geotechnical Engineering Office, Civil Engineering and Development Department, Hong Kong SAR, China

[5] Head, Geotechnical Engineering Office, Civil Engineering and Development Department, Hong Kong SAR, China

*Corresponding author (e-mail: hliubc@connect.ust.hk).

ABSTRACT: Boulders entrained in debris flow induce high impact forces on a rigid barrier. In current design practice, the concentrated load from boulders is estimated using the Hertz equation with a load reduction factor (K_c). Separately, the distributed load from the debris is estimated using the hydrodynamic equation. The existing design practice is simply adding the estimated loads using the two equations. The interaction between debris flow and boulders during the impact process is neglected. In this study, physical tests were conducted using a newly-developed 28-m-long flume to shed light on the impact dynamics of debris flows with and without boulders on an instrumented rigid barrier. Contrary to existing design practice where the boulder and debris impact loads are added together, the debris provided a cushioning effect to attenuate the impact force of the boulders. This cushioning effect was governed by a reflection wave with a length scale L_R/d (where d is the boulder diameter), which serves as cushioning thickness upon impact. L_R/d from 0.4 to 2.0 can reduce the impact load by up to 80% compared to existing design practice (K_c = 0.1).

(**Words:** 182)

Keywords: debris flows; boulders; boulder-enriched flows; impact; rigid barrier; physical modelling

Introduction

Concentrated impact loads induced by boulders entrained in debris flows are a crucial consideration when designing rigid barriers (Hungr et al. 1984; Zeng et al. 2015; Ng et al. 2016; 2018; Choi et al. 2016; Lam et al. 2018). Design guidelines generally neglect the interaction between debris flow and boulders. The distributed load from the debris flow is simply added to the concentrated loads from the boulders (Hungr et al. 1984; NILIM 2007; Kwan 2012). However, in reality, the viscous forces exerted by the debris flow on boulders may play an integral role in the total impact load.

A literature review on existing approaches to estimate the impact force induced by debris flow and boulders is carried out to reveal the current knowledge gap in predicting the impact force exerted by boulder-enriched debris flows. A hydrodynamic approach (Hübl et al. 2009; Armanini et al. 2011), which is based on the conservation of momentum, is most widely used to estimate the distributed load induced by debris flow:

$$F = \alpha\rho v^2 hw \tag{1}$$

where α is a pressure coefficient, ρ (kg/m^3) is the density of the flow, v (m/s) is the flow velocity, h (m) is the flow depth and w (m) is the channel width. To account for the simplifications and assumptions in Eq. (1), design guidelines often prescribe higher values of α to Eq. (1) for design robustness. For example, Kwan (2012) recommends an α of 2.5 for the design of rigid barriers to consider hard and large inclusions in the debris flow.

Eq. (1) treats a complex debris flow mixture as an equivalent fluid (Hungr 1995), meaning that the distinction between boulders and debris flow is not explicitly made. Since boulders induce concentrated impact loads over a tiny contact area, appropriate mechanics are needed to describe the involved contact between a sphere and a plane. To achieve this, the elastic Hertz equation may be used to estimate the impact load, F_b, induced by a boulder (VanDine 1996; SWCB 2005; Kwan 2012) as follows:

$$F_b = K_c n a^{1.5} \tag{2}$$

$$n = \frac{4 r_b^{0.5}}{3\pi(k_b + k_B)} \tag{3}$$

$$a = \left(\frac{5 m_b v_b^2}{4n}\right)^{0.4} \tag{4}$$

$$k_b = \frac{1 - \mu_b^2}{\pi E_b} \tag{5}$$

$$k_B = \frac{1 - \mu_B^2}{\pi E_B} \tag{6}$$

where K_c is a load reduction factor, which is recommended to be 0.1 to compensate for plastic deformation during impact (Hungr et al. 1984; Lo 2000; Sun et al. 2005; Kwan 2012). Variables r, m, v, μ and E are radius (m), mass (kg), impact velocity (m/s), Poisson's ratio and elastic modulus (Pa), respectively. Subscripts "b" and "B" correspond to the boulder and barrier, respectively.

Song et al. (2018) carried out two series of centrifuge tests to study the impact behaviour of idealised dry mono-disperse boulder flows with and without sand on a rigid barrier. The prototype diameter of the boulders was varied from 70 mm to 870 mm. Their experimental findings showed that as the size of the boulders increased, transient impulses generated by these boulders governed the overall design load. Moreover, it was reported that if Eq. (1) is used to estimate the boulder impact force, then an α of 2.5 can be used safely determine the impact force for boulders with a diameter that is up to 0.6 times the flow depth before impact. However, their experiments were conducted using dry granular flows, which are fundamentally different compared with debris flows. For debris flows, both the solid and fluid phases play integral roles in regulating the mesoscopic and macroscopic flow dynamics (Iverson 2015; Ng et al. 2017; Song et al. 2017; Zhou et al. 2018; Song et al. 2018). More importantly, the inertial and static fluid stresses (Alexander and Cooker 2016) that transport boulders for debris flow are fundamentally different compared to that of dry granular flow.

In this study, boulder flows, and debris flows with and without boulders were modelled to investigate the impact mechanisms of boulder-enriched debris flow on a rigid barrier using a newly-developed 28-m-long flume model. Impact characteristics for different flow compositions and the effects of debris flow cushioning on boulder impact are examined.

Twenty-eight-meter-long Flume Modelling

Fig. 1 shows a plan view of the flume model and instrumentation used in this study. The channel has a total length of 28 m, a width and depth of 2 m and 1 m, respectively. The storage tank has a maximum volume of 10 m^3. The tank occupies the upper 5 m of the channel, which is inclined at 30°. Just downstream from the storage tank is a 15-m-long channel section that is inclined at 20°. At the end of the inclined channel is an 8-m-long horizontal channel section. A mechanical arm, controlled using an electric motor, was used to retain and release the dual gates.

An *L*-shaped reinforced concrete barrier (Fig. 2) was constructed and positioned at the mouth of the inclined section of the channel. The barrier has a height, width, and thickness of 1.8 m, 1.9 m, and 0.3 m, respectively. Four load cells were sandwiched between a stainless-steel force plate and the reinforced concrete barrier to measure the impact load. The stainless-steel plate has a height, width and thickness of 1480 mm, 1900 mm, and 20 mm, respectively. The barrier weighed a total of 4.5 tons and was constructed on a 100-mm-thick layer of compacted soil. At the base of the *L*-shaped barrier, two instrumentation cells (discussed below) were installed to measure the debris flow properties.

Instrumentation

Fig. 3 shows a typical instrumentation cell installed at the base of the flume to obtain measurements of the model debris flow. The frame of the instrumentation cell was constructed using stainless-steel (Fig. 3a). At the top of the frame was a circular opening for a polyvinyl chloride (PVC) plate with a diameter of 0.32 m to transfer loading to a load cell, which was used to measure the basal stresses induced by the debris flow. The load cell rested on a cross beam supported by the stainless steel frame (Fig. 3b). The PVC plate had two openings with meshes (to filter fines) to enable the measurement of changes in pore water pressure. Two cylindrical chambers constructed using aluminium with a diameter of 0.10 m and a height of 0.05 m were connected to each opening on the PVC plate. On the side of the cylindrical chambers, an opening was provided to connect pore pressure transducers to measure changes in pore pressure (Fig. 3c). Before each test, each cylindrical chamber was filled with water. When debris flow passed over the PVC plates, basal stresses and excess pore pressures generated by the debris flow were measured by each instrumentation cell.

Fig. 4 shows a side schematic of the test setup. Five instrumentation cells (Cells 1 to 5) were installed at the base of the channel to measure the debris flow properties. A laser sensor was mounted above the centre of Cell 4 and another laser sensor was installed 1.5 m upstream from the centre of Cell 3. Four piezo-resistive load cells were sandwiched between the force plate and the reinforced concrete *L*-shaped barrier to measure the total impact force exerted by the debris flow. A high-speed camera was installed on top of the *L*-shaped barrier. The high-speed camera recorded images at 300 frames per second (fps) with a resolution of 2336 × 1728 pixels. The images were used to deduce the velocities of the flow and boulders before impact. Additionally, a video camera was installed above Cell 3. This video camera was installed facing the *L*-shaped barrier. The video camera recorded images at 120 fps with a resolution of 1920 × 1080 pixels. An unmanned aerial vehicle was used to capture a bird's eye view of the entire test to record images at 30 fps with a resolution of 1920 × 1080 pixels.

Test Programme and Test Procedures

In total, four tests were conducted. A debris flow with a volume of 2.5 m^3 (test D) and a same volume of debris flow with ten boulders (test DB10) were modelled. Furthermore, tests with single and ten boulders were also conducted. The test programme is summarised in Table 1.

The boulders in each test were placed at the base of the storage tank behind the gate. For the single boulder, the granite sphere was placed in the middle of the tank behind the gate. For ten boulders, the granite spheres were placed in a line at the base of the storage tank (Fig. 4). The boulders in this study were modelled using spherical granite with a diameter d of 200 mm. The debris material composed of gravel, sand, clay, and water with volumetric fractions of 0.21, 0.36, 0.02 and 0.41, respectively. The gravel and sand had typical sizes of 20 mm and 2 mm, respectively. The clay adopted was kaolin clay with a particle size smaller than 0.006 mm. Details of the debris composition are summarised in Table 2.

Before each test, the debris material was well mixed by a truck mixer and transported into the storage container to reach the target volume. After the preparation of test material in the container, data logger and cameras were triggered and the mechanical arm was lifted to release the gate.

Flow Characterisation

The Froude number is a ratio between the inertial force and gravitational force of the flow in a channel and is expressed as follows:

$$Fr = \frac{v}{\sqrt{gh\cos\theta}} \tag{7}$$

where g is the gravitational acceleration (9.81 m/s^2 in this study) and θ is the flume inclination (°). The Froude number has been recognised as a key parameter that governs the impact dynamics of open-channel flow (Hübl et al. 2009; Armanini et al. 2011; Choi et al. 2019). In this study, the Froude number of the flow before impacting the barrier ranges from 7.4 to 7.9, indicating that the inertial component is more dominant than the gravitational component of the flow and therefore dynamic loading is more significant (Faug 2015; Sovilla et al. 2016).

A New Equation to Estimate Boulder Impact with Debris Cushioning

Debris flows arrested by a rigid barrier may act as a cushion to attenuate the impact energy of incoming boulders as the debris reflects from the barrier to the upstream direction. In this section, a new approach is proposed to predict the boulder impact force by explicitly considering debris-boulder interaction.

Fig. 5 shows a schematic of boulder motion in a debris flow. When a boulder is entrained in a flow, the boulder is subjected to a gravitational force, $m_b g$, frictional force between the boulder and the flow bed, F_f, and drag force from the flow, F_d. A mathematical equation to describe the boulder motion is expressed as follows:

$$\frac{dv_m}{dt} = g\sin\theta - \frac{F_f}{m_b} + \frac{F_d}{m_b} \tag{8}$$

where v_m is boulder velocity (m/s) during motion and t is the time (s) after the gate has been opened. By assuming mainly translational motion, the frictional force F_f can be simplified as follows:

$$F_f = -\mu m_b g\cos\theta \tag{9}$$

where μ is the interface friction coefficient between the boulder and channel bed. Assuming the boulder is fully submerged in the flow, the drag force F_d on the boulder is exerted by the flow and is proportional to the square of the relative velocity between the flow and boulder (Alexander and Cooker 2016), which is expressed as follows:

$$F_d = \frac{1}{2} C_d A \rho \delta v^2 \tag{10}$$

where C_d is the drag coefficient, A is the cross-sectional area of the boulder in the plane perpendicular to the flow, ρ is the flow density and δv is the relative velocity of flow and boulder. When the flow velocity v is larger than the boulder velocity v_m, the drag force is in the same as the direction as the flow. When the flow velocity v is smaller than the boulder velocity v_m, the drag force is opposite to that of the flow direction. Substituting Eqs. (9) and (10), Eq. (8) can then be expressed as follows:

$$\frac{dv_m}{dt} = g \sin\theta - \mu g \cos\theta + \frac{C_d A \rho \delta v^2}{2m_b} \tag{11}$$

Eq. (11) neglects the force from boulder-boulder interaction, which is reasonable for debris flows with a low boulder fraction. For flow that has a high boulder fraction, interaction forces of boulder-boulder and boulder-flow should also be taken into account.

By obtaining the boulder velocity when impacting the barrier with Eq. (11), the boulder impact force can be calculated by using the Hertz equation [Eqs. (2) to (6)]. The stainless-steel force plate and granite boulders adopted in this study have Young's moduli of 200 GPa and 50 GPa, and Poisson's ratios of 0.3 and 0.2, respectively. Substituting the material properties into Eqs. (2) to (6) yields:

$$F_b = 6100 K_c v_b^{1.2} r_b^2 \tag{12}$$

The debris cushioning effect on boulder impact is mainly attributed to the attenuation of the boulder impact velocity, v_b. A reduced load reduction factor K_c can be expressed as follows:

$$K_c = 0.1\left(\frac{v_b}{v_0}\right)^{1.2} \tag{13}$$

The boulder velocity attenuation by the arrested debris is schematically shown in Figs. 6a and 6b. Fig. 6a shows a debris flow front just as it reaches the barrier. The relative distance between the debris flow and boulder fronts is given as δx. After the debris impacts the barrier, the arrested debris forms a reflection wave (Fig. 6b) with a height of h_j. This wave propagates in the upstream direction with a speed of v_r. Before impacting the barrier, the boulder first interacts with the reflection wave with length L_R (Fig. 6b), which serves as a cushioning thickness and dissipates the energy of the incoming boulder. The velocity of the boulder, v_b, when impacting the barrier is then reduced compared with its initial velocity, v_0, before interacting with the reflection wave.

After the boulder enters into the reflection wave, the drag force, F_d, exerted by the flow can be calculated by Eq. (10). An assumption that the flow is uniform and homogeneous, and that the motion of the boulder can be idealised as translational motion along a smooth channel bed is made. As the drag force from the flow becomes more significant than that of the frictional force from the flow bed, only the drag component is considered to influence the boulder velocity for simplicity. The impact velocity of the boulder, v_b, is given as follows:

$$v_b = v_0 e^{-0.75C_d\frac{\rho L_R}{\rho_b d}} \tag{14}$$

Substituting Eq. (14) into Eq. (13), the load reduction factor considering the cushioning effects provided by viscous damping can be expressed as follows:

$$K_c = 0.1e^{-0.9C_d\frac{\rho L_R}{\rho_b d}} \tag{15}$$

The drag coefficient C_d in Eqs. (14) and (15) can be taken as unity for a blunt body (Alexander and Cooker 2016). The boulder density ρ_b equals to 2800 kg/m^3, which was obtained from the measured boulder mass. More details on Eq. (14) are given in Appendix A.

Interpretation of Test Results

Observed Flow Kinematics

The time history of flow-front position has been adopted by Iverson et al. (2010) to describe the debris flow mobility. Fig. 7 shows the time histories of the flow-front position of the boulders and debris flow as captured by the video camera mounted on the unmanned aerial vehicle. The flow-front position is characterised relative to the distance from the gate of the storage tank and is expressed as s. The acceleration of a point mass is shown in Eq. (11). By neglecting the drag force, the theoretical flow distance s of a point mass can be expressed as following:

$$s = \frac{g \sin\theta - \mu g \cos\theta}{2} t^2 \tag{16}$$

When flow is on the inclined portion of the channel, θ = 20º, and when flow is on the depositional area, θ = 0º. The test with a single boulder (test B1) and test with ten boulders (test B10) had similar time histories of the flow-front position because the small amount of boulders induced insignificant boulder interactions. Considering a friction coefficient μ = 0.1, Eq. (16) can well estimate the boulder motion in the pure boulder tests (tests B1 and B10). This implies that assuming a pure translational motion is not an unreasonable approach to idealise the boulder motion in this study.

The test with just debris flow (test D) and the test with a mixture of debris flow and boulders (test DB10) exhibited similar kinematics at the debris front. For both test D and test DB10, the debris fronts accelerated 0.5 s after the opening of the gate and achieved a near constant velocity of about 6 m/s along the inclined section of the channel. When the debris reached the end of the inclined section of the channel, the flow decelerated by about 10% just before impacting the L-shaped barrier. The debris fronts for only debris flow (test D) and debris flow with ten boulders (test DB10) always remained ahead of flow fronts for pure boulder tests (tests B1 and B10) before impacting the barrier. This was because the debris front was driven by both its self-weight and the earth pressure in the flow direction (longitudinal direction) and can be quantified by a simplified depth-averaged momentum equation. The depth-averaged momentum equation was first proposed by Savage and Hutter (1989) and later widely adopted to describe the motions of both dry granular flows (Gray et al. 1999; Gray and Ancey 2011) and debris flows (Iverson 1997; Iverson et al. 2010; Johnson et al. 2012; Iverson and George 2014). A simplified depth-averaged momentum equation can be expressed as follows:

$$\frac{du}{dt} = g \sin\theta - \mu g \cos\theta - k \frac{\partial h}{\partial x} g \cos\theta \tag{17}$$

where u is the depth-averaged flow velocity (m/s) parallel to the channel bed, k is the longitudinal earth pressure coefficient, and x is downslope distance (m). In Eq. (17), the term du/dt is the acceleration at an arbitrary location of the flow mass, $g \sin\theta$ represents the translational motion downslope, $\mu g \cos\theta$ represents the basal frictional resistance, and $k(\partial h/\partial x) g \cos\theta$ characterises the longitudinal earth pressure within the flow mass. The term $k(\partial h/\partial x) g \cos\theta$ is negative within the head of the flow mass as the flow depth gradually decreases along the flow direction within the flow head. Therefore, the longitudinal earth pressure can increase the acceleration du/dt and accelerate the flow head, leading to a higher velocity than the boulders entrained in the flow. The flow distance for a frictionless point mass (μ = 0.0) calculated by Eq. (16) is shown in Fig. 7. The time history of this flow distance underestimates the measured motion of debris fronts for both debris flow test (test D) and the test of debris flow with ten boulders (test DB10). The underestimation may be attributed to the larger longitudinal pressure compared with the basal friction as expressed in Eq. (17). This caused a larger acceleration than the acceleration of a frictionless point mass $g \sin\theta$. Eq. (16) with μ = 0.0 overestimates the motion of boulder front when there is no debris flow but underestimates the motion of boulder front when boulders are entrained in debris flow. The overestimation may be mainly caused by the deceleration of the boulder motion due to basal friction. The underestimation may be mainly attributed to the acceleration of the boulder motion due to the drag force from debris flow as expressed in Eq. (11).

The movement of the boulders observed in this study was different compared with the kinematics of particle-size segregation (Jullien and Meakin 1990; Makse et al. 1997; Jing et al. 2017), whereby coarse particles usually segregate to the flow surface by kinetic sieving and are transported to the flow front by shear stress of the flow (Johnson et al. 2012). In this study, the flow maintained a high pore pressure that liquefied the flow. Therefore, the flow cannot lift the boulders because the boulders were more than twice of the flow depth and the density of the boulder was 1.4 times the bulk density of the flow. The movement of the boulder was then dominated by the drag force of the flow on the boulders. Under this circumstance, when boulders are entrained by the debris flow along the flow path, the boulders may move slower than the debris front and impact the barrier after the debris front. The first arrested debris can then form a cushioning layer to dissipate the boulder energy before impact. It should be noted that the transportation distance of debris flow can also affect the process of particle-size segregation. With a much longer transportation distance in the field, coarse particles may tend to segregate to the flow front when flows are not liquefied (Zhang et al. 2011).

The high pore pressure maintained in the debris flows was mainly attributed to the clay content (Iverson 1997; Iverson et al. 2010). Fig. 8 shows the comparison of liquefaction ratios, which is the ratio between the pore water pressure u_w and the total normal stress σ, with different clay contents. The liquefaction ratios for pure debris flow (test D) and debris flow with ten boulders (test DB10) at the location of Cell 4, which was 0.9 m away from the force plate, were measured. The measured liquefaction ratios for both test D and test DB10 were close to unity and pore water pressures were about 1.6 times that of hydrostatic conditions when the debris flows deposited behind the barrier. The high pore pressures mean that the flows were nearly liquefied and the grain contact stresses were minimal. Similarly, Iverson et al. (2010) reported that their flows remained liquefied even after deposition. Liquefied flows were especially pertinent for flows with high clay (particle size < 0.0625 mm) content. In contrast, flows with lower clay contents (less than or equal to 1% reported by Iverson et al. 2010) resulted in higher effective stresses. Therefore, the clay content plays an important role in generating excess pore pressures in debris flows. Observations from vertically rotating drum tests by Kaitna et al. (2016) also showed an increasing trend of the liquefaction ratio for steady-state flows with increasing clay content. The clay content in a debris flow maintains pore pressure by decreasing the permeability of the pore water. A decreased permeability can lead to an estimated time of 4000 s to dissipate the pore pressure for a depth of 0.1 m (Major et al. 1997; Major 2000; Iverson et al. 2010). The liquefied flow conditions also imply that a hydraulic approach can be adopted to estimate the impact loads of the debris deposits.

Fig. 9 shows the observed impact kinematics of the debris flow only (test D) and the debris flow with ten boulders (test DB10). When the debris flow impacted the barrier, the flow jumped along the face of the barrier (Fig. 9a) and was immediately reflected back upstream (Fig. 9b). As the reflected wave propagated to upstream (Fig. 9c), it interacted with the incoming flow that had not yet impacted the barrier. Eventually, the debris deposited and reached a static state with a horizontal surface (Fig. 9d). The horizontal deposition profile implies that a zero deposition angle can be reached when debris flow is in a liquefied condition. For boulder-enriched debris flows, the debris front arrived at the barrier earlier than the boulders (Fig. 9e). After the debris front impacted the barrier, the two boulders at the flow front impacted the barrier (Fig. 9f). As more debris arrested by the barrier and reflected upstream by the barrier, incoming flow and boulders impacted on the reflected debris flow (Figs. 9f ~ 9h). In essence, the reflected debris flow provided a cushioning effect for incoming boulders. At the end of the impact process, all the boulders were buried in the deposited debris material and a same deposition profile as shown in Fig. 9d was obtained. The observed kinematics of the boulder-enriched debris flows demonstrated that boulders may not necessarily be segregated to flow front due to their much larger size compared to the flow depth and the liquefied flow condition. The earlier arrested debris material by the barrier can form a cushioning layer via viscous damping, which dissipates the impact energy of the subsequent boulders.

Impact Force of Debris Flow

Fig. 10 shows a comparison of the time histories of the measured total impact force of debris flow (test D) and debris flow with ten boulders (test DB10). To examine the complex impact dynamics of boulder-enriched debris flows, we first look into the impact load exerted by a debris flow only. At t = 3.0 s, the debris impacted the barrier. The total force exerted on the barrier reached a peak load at t = 4.4 s. The total force gradually decreased until t = 7.3 s and reached a static state. The impact force is normalised by a theoretical impact force calculated by Eq. (1) with α = 1.0. The density used to calculate the impact force is deduced from the measured peak normal stress and flow depth at Cell 3 (Fig. 4), which was located 4.4 m upstream from the barrier. The measured density was 1870 kg/m^3, which was about 5% lower than the initial debris density (1960 kg/m^3). The impact velocity is taken as the average velocity of the flow front before impacting the barrier. The pre-impact velocity was measured from the high-speed camera. The flow depth was measured by laser sensor 2 (Fig. 4) at the time that the flow impacts the barrier to avoid the influence of the reflected debris material. With the accurate measurements of the flow density, impact velocity and flow depth, the measured peak force is well-captured by the hydrodynamic equation when α is unity.

Higher α values are usually suggested by international design guidelines (Kwan 2012; Volkwein 2014; Vagnon and Segalini 2016) to consider the influence of hard inclusions and different debris flow types. However, the largest particle of the debris material in this study was only 20 mm, which did not induce obvious impulses. Moreover, measurements from the instrumentation cells in Fig. 8 show that debris flow impact in this study was an undrained process due to the high rate of loading and low permeability of the debris material. The nearly-liquefied state induces less energy dissipation during impact compared with that of dry granular flows, which readily dissipate flow kinetic energy as grains shear and the granular assembly compresses (Ng et al. 2017). The liquefied flow may also be the reason that an equivalent fluid approach is suitable for predicting the impact load of a debris flow. By treating debris flow that can maintain high excess pore pressure as an equivalent fluid, the major remaining challenge in estimating the impact load is the effects caused by the large and hard inclusions, which generate sharp impulses during impact.

Impact Force of Boulder-enriched Debris Flow

The force-time history for debris flow with ten boulders (test DB10) shows that the debris acted as a cushion for the boulders in the flow. Subsequent impulses generated from boulder impact were dampened as the volume of debris flow arrested by the barrier increased. The cushioning mechanism was caused by the viscous shear resistance between boulders and the pore fluid and the shear resistance between the boulders and the finer solid particles in the debris flow. By comparing the time history of pure debris flow impact with the boulder-enriched debris, it can be observed that the sharp impulses were induced by the boulders. The peak load occurred at t = 2.9 s and was caused by a combination of the debris flow loading and boulder loading. After the peak impulse occurred, four additional impulses with normalised impact forces ranging from 2.1 to 2.7 were caused by the other boulders in the flow. Additionally, impulses with normalised forces from 1.2 to 1.3 were observed from t = 3.8 s to t = 4.1 s. Decomposing the total impact force gives normalised boulder impact forces of about only 0.2 (from t = 3.8 s to t

= 4.1 s). The normalised impact force from the debris increased until it reached a peak load, which was 1.1, at t = 4.2 s. Afterwards, the impact force decreased gradually until a static state was reached at t = 7.1 s.

The hydrodynamic impact model [Eq. (1)] with an α of 1.0 cannot capture the peak impulses from boulder impact but still can capture the peak load induced by the debris flow. By comparing the results predicted using Eq. (1) with an α of 2.5 (Kwan 2012), the peak load is still underestimated by more than 50%, bearing in mind that the recommended design value by Kwan (2012) explicitly considers hard inclusions in the debris flow. This is because the fundamental assumptions behind Eq. (1) and Eqs. (2) ~ (6) are different. The hydrodynamic equation treats the complex debris flow as an equivalent fluid (Hungr et al. 1984), which exerts a force distributed over a finite area. In contrast, the Hertz equation (Johnson 1985) assumes a concentrated elastic impact between a sphere and a plane over a very small contact area. Therefore, only significantly higher α values in the hydrodynamic equation can explicitly capture the effects of boulder impact. However, this has practical limitations. The underestimation of the loading induced by boulder-enriched debris flow by Eq. (1) highlights the uncertainty in using α (Zhang 1993; Kwan 2012; Vagnon and Segalini 2016). For boulder-enriched debris flow, the hydrodynamic impact model should be used to estimate the debris impact force, while the Hertz equation still needs to be used to estimate the boulder impact force. A criterion that can distinguish between boulder and debris is recommended by Song et al. (2018). They recommended a ratio of boulder diameter to flow depth, d/h, where particles with a size $d/h \geq 0.6$ can be regarded as boulders. To determine the impact forces for boulder-enriched debris flow, however, a K_c value considering the effects of viscous damping of the debris flow can provide further optimisation of designs.

Performance of the Newly-proposed Equation for Estimating Debris Cushioning on Boulder Impact

Fig. 11 shows the load reduction factors, K_c, resulting from different lengths of debris reflection wave (Fig. 6b) normalised by boulder diameter, L_R/d. The length of the reflection wave serves as a cushioning thickness to dissipate boulder impact. The high-speed camera, which was mounted on top of the barrier (Fig. 4), was adopted to capture L_R and the velocities of boulders upon interacting with the reflection wave. The boulder impact forces for debris mixed with ten boulders (test DB10) are extracted from Fig. 10 by removing the loads induced from the debris and by only considering the transient impulses. The K_c values of the tests using a single boulder (test B1) and ten boulders (test B10) are shown for comparison and are both found to be close to the recommended K_c value of 0.1 in the literature (Hungr et al. 1984; VanDine 1996; Kwan 2012). This is because the lengths of debris reflection wave were equal to zero, and thus there was no cushioning effect from the debris. The measured K_c from the test with ten boulders without debris (test B10) is found to be 10% larger than the recommended design value 0.1. This is attributed to two boulders impacted the barrier at almost the same time (impact interval was less than 0.03 s from the unmanned aerial vehicle images). The calculated $K_c = 0.11$ for the test with ten boulders without debris (test B10) implies that a higher than the recommended K_c of 0.1 may be needed to account for the possible superposition of boulder impact loads when $L_R/d = 0$. Meanwhile, superposition of the debris flow impact load should also be carried out.

When $L_R/d > 0$, debris reflection was formed before boulder impacting the barrier. K_c decreases sharply and keeps decreasing with an increasing L_R/d because more boulder energy was dissipated by the enlarging debris reflection wave. In addition, L_R/d values from 0.4 to 2.0 lead to a K_c that is up to 80% lower compared to the K_c of 0.1. At a distance of $L_R/d \geq 2.7$, K_c is approximately zero. Evidently, the length of debris reflection wave contributes to attenuating the boulder impact force.

Calculated K_c values using Eq. (15) as a function of the normalised debris reflection length, L_R/d are shown. K_c values are significantly affected by the density of the flow. When the flow is considered to be air (dry granular flow), the calculated K_c value is equal to the suggested value by design guideline (Kwan 2012). A flow density equals to that of pure water may overly estimate the K_c values. By applying a flow density of 1960 kg/m^3, which was the initial debris flow density, Eq. (15) can reasonably estimate the load reduction factor K_c and provide an upper bound for the measured K_c. Overestimating K_c may because Eq. (15) simplifies the debris reflection as a uniform and homogenous fluid and neglects the interaction between boulder and the debris solid fraction, which is about 60% of the total flow volume. In addition, only drag force is considered by Eq. (15) for cushioning the boulder impact. However, cushioning material in front of the rigid barrier has been reported can change the load spreading process, which further attenuates the load transmitted to the barrier (Ng et al. 2018; Su et al. 2019). Nevertheless, Eq. (15) well estimates the decreasing trend of K_c with the increase of reflection wave length and is capable of providing a first approximation on K_c to quantify the cushioning effect from viscous damping.

It should be noted that spherical boulders with a uniform diameter were adopted in this study to easily characterise boulder kinematics and dynamics without the influence of different boulder sizes and shapes. The proposed Eq. (15) assumes that the diameter of the boulder d is smaller than the thickness of the reflection wave h_j as shown in Fig. 6b. It is expected that the proposed Eq. (15) holds for boulders with a diameter $d < h_j$ because this diameter is consistent with the assumptions made by Eq. (15). Song et al. (2018) recommended that Eqs. (2) ~ (6) should be adopted to estimate the boulder impact force for boulders that have a diameter larger than 0.6 times of the flow depth h. Therefore, boulder with a diameter $0.6h < d < h_j$ is recommended for adopting Eq. (15). For a small boulder that has a size approaching 0, the L_R/d approaches infinity, the cushioning effect of the reflected debris on the boulder is very significant and boulder impact force can be neglected. For this condition, K_c equals to 0 as calculated by Eq. (15). The impact force of the debris flow can be calculated by only using the continuum approach, such as the hydrodynamic equation [Eq. (1)]. For boulder that has a diameter larger than h_j, the effects of viscous damping may be reduced due to the smaller contact area compared with the area that a boulder is fully immersed in the flow. Notwithstanding, a $K_c = 0.1$ would still be adopted to provide a conservative prediction. When $d \gg L_R$ and L_R/d approaches 0, the cushioning effect from the reflected debris can be neglected due to the negligible cushioning thickness and K_c should be taken as 0.1 to estimate the boulder impact force in a debris flow.

The proposed Eq. (15) does not consider the effects of the number of boulders on load reduction factor K_c. In this study, the performance of the Eq. (15) is only verified by debris flow that entrained ten spherical boulders with a boulder fraction of up to 2% of the debris flow volume. For debris flows with a much larger number of boulders and a much higher boulder fraction, the frictional and collisional stresses among boulders may be more prominent than the damping provided by the debris flow. Therefore, the proposed equation may be required to be modified for a much higher boulder fraction. A further investigation of the effects of boulder fractions on the impact dynamics of boulder-enriched debris flow is still warranted.

In this study, the Hertz model together with an empirical coefficient that implicitly considers plastic deformation was adopted to estimate the boulder impact force. It is worthwhile to mention that there are also analytical models that can explicitly consider the plastic deformation during boulder impact (Yigit et al. 2011; Brake 2012; Ma and Liu 2015). These methods usually require information on the evolution of the plastic regions (Ma and Liu 2015). However, difficulty in measuring such data has hindered a well-accepted approach that considers plastic deformation. Wang et al. (2020) summarised 18 theoretical elastoplastic contact models and found that the definition of the yield condition during loading phase is necessary for an accurate prediction of the impact. Evidently, a further investigation of the yield criterion for boulder impact on barriers would enhance a more rational approach for estimating boulder impact force. Nevertheless, the more pragmatic engineering approach with an empirical coefficient K_c as expressed in Eqs. (2) ~ (6) has the merit of being simple and robust enough for engineering design and is currently widely adopted in engineering practice internationally (SWCB 2005; NILIM 2007; Kwan 2012).

Implications for Designing Debris-resisting Barriers in Practice

The impact dynamics of debris flow against debris-resisting barriers are not well understood because of the heterogeneous nature of debris flows and the idiosyncrasies of the natural settings involved. Therefore, to ensure a conservative barrier design, the above-mentioned factors should be considered. To highlight the general dearth of knowledge in estimating boulder impact, an empirical load reduction factor of 0.1 is required to reduce the impact load predicted using the elastic Hertz equation [Eq. (12)]. Kwan (2012) suggested that if simultaneous boulder impact may occur, the design impact load per meter run of the barrier should be taken as the impact load of the largest boulder divided by the boulder diameter. Following this approach, the total design impact load for the rigid barrier is 650 kN, which is 23 times higher than the measured peak impact load for debris flow with ten boulders from the physical experiments in this study (Fig. 10; test DB10). Evidently, there is room to enhance our understanding and to optimise the current design load of boulder-enriched debris flows.

Aside from the complexities attributed to the debris flow itself and the natural terrain, different types of debris-resisting barriers may also result in entirely different impact processes and dynamics. The results in this study are for a fully closed rigid barrier without overflow or barrier deformation. For open structures, such as baffles (Choi et al. 2015; Law et al. 2015; Ng et al. 2015) and slit dams (Choi et al. 2016; Zhou et al. 2019), debris may discharge through and around these structures and the cushioning effect identified in this study may not be as prominent as compared with that for closed barriers. For flexible barriers (Wendeler and Volkwein 2015; Wendeler et al. 2019; Song et al. 2019), the deformation of the barrier may lead to a different debris reflection compared with rigid barriers and alter the boulder-flow-barrier interaction process. To further rationalise the design of debris-resisting barriers in practice, advanced numerical modelling methods together with high quality physical data can potentially optimise the resisting capacity required by a barrier.

In engineering design practice, well calibrated numerical models are utilised to optimise designs. For instance, a depth-averaged continuum numerical software 2d-DMM (Kwan and Sun 2006; Law and Ko 2018) and a finite element software package LS-DYNA (Crosta et al. 2003) have been recommended by design guidelines (Kwan 2012; Koo 2017) to obtain the design velocity and flow depth to estimate impact loads. Koo (2017) also recommended the use of LS-DYNA to model the impact dynamics of flow against rigid (Ng et al. 2018) and flexible (Koo and Kwan 2014; Cheung et al. 2018) barriers. Although LS-DYNA can also model boulder impact (Koo and Kwan 2014; Ng et al. 2018), a deficiency of unique reliable large-scale data has hindered model calibration. The findings from this study stress the importance of modelling the debris and boulder separately for the design of barriers. More recently, coupled approaches using the discrete element method with computational fluid dynamics have been reported (Li and Zhao 2018). However, the computational cost for such an approach limits its use for larger scale problems in practical engineering design. The observed importance of capturing the boulder and debris loads separately in this study further suggests that more advanced numerical approaches are needed to advance the state-of-the-art and rationalise the design of debris-resisting barriers.

Conclusions

A series of 28-m long flume tests has been conducted to highlight the interaction between the debris flow and boulders on the impact behaviour against rigid barriers. The results from this study were based on a debris flow mixture of gravel, sand, clay and water with volumetric fractions of 0.21, 0.36, 0.02 and 0.41, respectively. The gravel and sand had average sizes of 20 mm and 2 mm, respectively. The clay had a particle size smaller than 0.006 mm. Boulders adopted by this study were spherical granite with a uniform diameter of 200 mm. Findings from this study may be drawn as follows:

a) Contrary to existing design practice where the boulder and debris impact loads are added to each other, the debris provides a cushioning effect to attenuate the impact force of the boulders.

b) For situations that debris flow front impacts on the rigid barrier prior to boulders coming behind, the reflection wave of debris flow propagates to upstream after debris front interacts with the barrier and provides a cushioning effect on the boulders. The enlarging reflection wave length could serve as a cushioning thickness with a length scale of L_R/d, where L_R is the reflection wave length upon interacting with each boulder and d is the boulder diameter. Measured boulder impact loads in this study show that L_R/d values from 0.4 to 2.0 can reduce the impact load by up to 80% compared to existing design practice ($K_c = 0.1$), and $L_R/d \geq 2.7$ can lead K_c approximately to zero.

c) A new equation has been proposed and evaluated to estimate the K_c values with consideration of debris cushioning effects based on different L_R/d ratios. The new equation can serve as a scientific basis for optimising design impact load for debris flow with a boulder fraction of up to 2% of the flow volume.

Data Availability Statement

All data, models, or code that support the findings of this study are available from the corresponding author upon reasonable request.

Acknowledgements

The work described in this paper was supported by a grant from the National Natural Science Foundation of China (51709052) and also financial sponsorships from the Research Grants Council of the Hong Kong Special Administrative Region, China (Project Nos. AoE/E-603/18, T22-603/15-N, 16212618 and 16209717). This paper is published with the permission of the Director of Civil Engineering and Development and the Head of the Geotechnical Engineering Office of the Hong Kong Special Administrative Region of China.

Appendix A: Derivation of Eq. (14)

The boulder is assumed only subjected to the drag force [Eq. (10)] after the boulder enters into the reflection wave (Fig. 6b). The acceleration of the boulder can be expressed as follows:

$$a(t) = -\frac{C_d A \rho \delta v^2}{2m_b} \tag{A1}$$

The mass of the spherical boulders as a function of the boulder cross-sectional area A can be expressed as follows:

$$m_b = \frac{2}{3}\rho_b d A \tag{A2}$$

Assuming the flow velocity inside the reflection wave is zero, then the relative velocity of boulder and flow, δv, can be represented by the boulder velocity as a function of time, which is $\delta v = v(t)$. The boulder velocity, $v(t)$, after boulder enters into the debris can be expressed as follows:

$$v(t) = v_0 + \int_0^t a(t)\,dt = v_0 - \frac{3C_d A\rho}{4\rho_b d}\int_0^t v^2(t)\,dt \tag{A3}$$

As shown in Fig. 6b, the transportation distance of the boulder from entering into the reflection wave to impacting the barrier is L_R, which can be obtained by integrating the $v(t)$ shown as follows:

$$L_R = \int_0^t v(t)\,dt \tag{A4}$$

Solve Eq. (A3) by taking the time derivative for both sides of the equation. With a boundary condition $v(0) = v_0$, substituting the resulting $v(t)$ into Eq. (A4) yields Eq. (14).

References

Alexander, J., and Cooker, M. J. 2016. "Moving boulders in flash floods and estimating flow conditions using boulders in ancient deposits." *Sedimentology 63*(6): 1582–1595. https://doi.org/10.1111/sed.12274.

Armanini, A., Larcher, M., and Odorizzi, M. 2011. "Dynamic impact of a debris flow front against a vertical wall." *In* Proceedings of the 5th International Conference on Debris-Flow Hazards Mitigation: Mechanics, Prediction and Assessment, Padua, Italy, pp. 1041–1049.

Brake, M. 2012. "An analytical elastic-perfectly plastic contact model." *Int. J. Solids Struct.* 49(22): 3129–3141. https://doi.org/10.1016/j.ijsolstr.2012.06.013.

Cheung, A.K.C, Yiu, J., Lam, H.W.K, and Sze, E.H.Y. 2018. "Advanced numerical analysis of landslide debris mobility and barrier interaction." *HKIE Transactions* 25(2):76–89. https://doi.org/10.1080/1023697X.2018.1462106.

Choi, C.E., Ng, C.W.W., Song, D., Law, R.P.H., Kwan, J.S.H. and Ho, K.K.S. 2015. "Computational investigation of baffle configuration on impedance of channelized debris flow." *Can. Geotech. J.* 52(2): 182–197. https://doi.org/10.1139/cgj-2013-0157.

Choi, C.E., Goodwin, G., Ng, C.W.W., Cheung, D.K.H., Kwan, J.S.H., and Pun, W.K. 2016. "Coarse granular flow interaction with slit-structures." *Géotechnique Letters* 6(4): 1–8. https://doi.org/10.1680/jgele.16.00103.

Choi, C. E., Ng, C. W. W., Liu, H., and Wang, Y. 2019. "Interaction between dry granular flow and rigid barrier with basal clearance: analytical and physical modelling." *Can. Geotech. J.* https://doi.org/10.1139/cgj-2018-0622.

Crosta, G.B., Imposimato, S., and Roddeman, D.G. 2003. "Numerical modelling of large landslides stability and runout." *Natural Hazards and Earth System Sciences* 3:523–538. https://doi.org/10.5194/nhess-3-523-2003.

Gray, J.M.N.T, Wieland, M., and Hutter, K. 1999. "Gravity driven free surface flow of granular avalanches over complex basal topography." *Proc. R. Soc.* A 455, 1841–1874. https://doi.org/10.1098/rspa.1999.0383.

Gray, J. M. N. T., and Ancey, C. 2011. "Multi-component particle-size segregation in shallow

granular avalanches." *Journal of Fluid Mechanics* 678, 535–588. https://doi.org/10.1017/jfm.2011.138.
Faug, T. 2015. "Depth-averaged analytic solutions for free-surface granular flows impacting rigid walls down inclines." *Physical Review E* 92, 062310. https://doi.org/10.1103/PhysRevE.92.062310.
Hübl, J., Suda, J., Proske, D., Kaitna, R., and Scheidl, C. 2009. "Debris flow impact estimation." *In* Proceedings of the 11th International Symposium on Water Management and Hydraulic Engineering, Ohrid, Macedonia, pp. 1–5.
Hungr, O. 1995. "A model for the runout analysis of rapid flow slides, debris flows, and avalanches." *Can. Geotech. J.* 32(4): 610–623. https://doi.org/10.1139/t95-063.
Hungr, O., Morgan, G.C., and Kellerhals, R. 1984. "Quantitative analysis of debris torrent hazards for design of remedial measures." *Can. Geotech. J.* 21(4): 663–677. https://doi.org/10.1139/t84-073.
Iverson, R.M. 1997. "The physics of debris flows." *Reviews of geophysics* 35(3): 245–296. https://doi.org/10.1029/97RG00426.
Iverson, R.M. 2015. "Scaling and design of landslide and debris-flow experiments." *Geomorphology* 244, 9–20. https://doi.org/10.1016/j.geomorph.2015.02.033.
Iverson, R.M., Logan, M., LaHusen, R.G., and Berti, M. 2010. "The perfect debris flow: aggregated results from 28 large-scale experiments." *J. Geophys. Res.* 115, F03005. https://doi.org/10.1029/2009JF001514.
Iverson, R.M., and George, D.L. 2014. "A depth-averaged debris-flow model that includes the effects of evolving dilatancy. I. Physical basis." *Proc. R. Soc.* A 470(2170): 20130819. https://doi.org/10.1098/rspa.2013.0819.
Iverson, R.M., George, D.L., and Logan, M. 2016. "Debris flow runup on vertical barriers and adverse slopes." *J. Geophys. Res.: Earth Surf.* 121(12): 2333–2357. https://doi.org/10.1002/2016JF003933.
Jing, L., Kwok, C.Y., and Leung, Y.F. 2017. "Micromechanical origin of particle size segregation." *Physical Review Letters 118*(11): 118001. http://doi.org/10.1103/PhysRevLett.118.118001.
Johnson, K.L. 1985. *Contact mechanics.* Cambridge University Press, London, UK.
Johnson, C.G., Kokelaar, B. P., Iverson, R.M., Logan, M., LaHusen, R.G., and Gray, J.M.N.T. 2012. "Grain-size segregation and levee formation in geophysical mass flows." *J. Geophys. Res.: Earth Surf. 117*, F01032. https://doi.org/10.1029/2011JF002185.
Jullien, R., Meakin, P. 1990. "A mechanism for particle size segregation in three dimensions." *Nature* 344, 425–427. https://doi.org/10.1038/344425a0.
Kaitna, R., Palucis, M.C., Yohannes, B., Hill, K.M., and Dietrich, W.E. 2016. "Effects of coarse grain size distribution and fine particle content on pore fluid pressure and shear behavior in experimental debris flows." *J. Geophys. Res.: Earth Surf.* 121(2): 415–441. https://doi.org/10.1002/2015JF003725.
Koo, R.C.H. 2017. *3D debris mobility assessment using LS-DYNA.* GEO Report No. 325. Geotechnical Engineering Office, Civil Engineering and Development Department, The HKSAR Government.
Koo, R.C.H., and Kwan, J.S.H. 2014. *A Numerical study of dynamic responses of two selected flexible rockfall barriers subject to punching and areal loads. Technical Note No. TN 4/2014*. Geotechnical Engineering Office, Civil Engineering and Development Department, The HKSAR Government.
Kwan, J.S.H. 2012. *Supplementary technical guidance on design of rigid debris resisting barriers.* Technical Note No. TN 2/2012. Geotechnical Engineering Office, Civil Engineering and Development Department, The HKSAR Government.
Kwan, J.S.H., and Sun, H.W. 2006. "An improved landslide mobility model." Canadian

Geotechnical Journal 43(5): 531-539. https://doi.org/10.1139/t06-010.

Lam, C., Kwan, J.S.H., Su, Y., Choi, C.E., Ng, C.W.W. 2018. “Performance of ethylene-vinyl acetate foam as cushioning material for rigid debris-resisting barriers.” *Landslides* 15(9): 1779–1786. https://doi.org/10.1007/s10346-018-0987-z.

Law, R.P.H., Choi, C.E. and Ng, C.W.W. 2015. “Discrete-element investigation of influence of granular debris flow baffles on rigid barrier impact.” *Can. Geotech. J.* 53(1): 179–185. https://doi.org/10.1139/cgj-2014-0394.

Law, R.P.H., and Ko, F.W.Y. 2018. *Validation of geotechnical computer program “2d-DMM (Version 2.0)”.* GEO Report No. 332. Geotechnical Engineering Office, Civil Engineering and Development Department, The HKSAR Government.

Li, X., and Zhao, J. 2018. “A unified CFD‐DEM approach for modeling of debris flow impacts on flexible barriers.” *International Journal for Numerical and Analytical Methods in Geomechanics* 42(14): 1643–1670. https://doi.org/10.1002/nag.2806.

Lo, D.O.K. 2000. *Review of natural terrain landslide debris-resisting barrier design.* GEO Report No. 104. Geotechnical Engineering Office, Civil Engineering and Development Department, The HKSAR Government.

Ma, D. and Liu, C. 2015. “Contact law and coefficient of restitution in elastoplastic spheres.” *Journal of Applied Mechanics* 82(12): 121006. https://doi.org/10.1115/1.4031483.

Major, J.J. 1997. “Depositional processes in large‐ scale debris‐ flow experiments.” *J. Geol.* 105, 345–366. https://doi.org/10.1086/515930.

Major, J.J. 2000. “Gravity□driven consolidation of granular slurries: Implications for debris□ flow deposition and deposit characteristics.” *J. Sediment. Res.* 70,64–83. https://doi.org/10.1306/2DC408FF-0E47-11D7-8643000102C1865D.

Makse, H.A., Havlin, S., King, P.R. and Stanley H.E. 1997. “Spontaneous stratification in granular mixtures.” *Nature* 386, 379–382. https://doi.org/10.1038/386379a0.

Ng, C.W.W., Choi, C.E., Song, D., Kwan, J.S.H., Koo, R.C.H., Shiu, H.Y.K., and Ho, K.K.S. 2015. “Physical modelling of baffles influence on landslide debris mobility.” *Landslides* 12(1): 1–18. https://doi.org/10.1007/s10346-014-0476-y.

Ng, C.W.W., Choi, C.E., Su, A.Y., Kwan, J.S.H., and Lam. C. 2016. “Large-scale successive impacts on a rigid barrier shielded by gabions.” *Can. Geotech. J.* 53(10): 1688–1999. https://doi.org/10.1139/cgj-2016-0073.

Ng, C.W.W., Song, D., Choi, C.E., Kwan, J.S.H., Koo, R.C.H., and Pun, W.K. 2017. “Impact mechanisms of granular and viscous flows on rigid and flexible barriers.” *Can. Geotech. J.* 54(2): 188–206. https://doi.org/10.1139/cgj-2016-0128.

Ng, C.W.W., Su, A.Y., Choi, C. E., Lam, C., Kwan, J.S.H., Chen, R., and Liu, H. 2018. “Comparison of Cushion Mechanisms between Cellular Glass and Gabions Subjected to Successive Boulder Impacts.” *Journal of Geotechnical and Geoenvironmental Engineering (ASCE)* 144(9): 04018058. https://doi.org/10.1061/(ASCE)GT.1943-5606.0001922.

NILIM. 2007. *Manual of technical standard for establishing sabo master plan for debris flow and driftwood.* Technical Note of NILIM No. 364. Natural Institute for Land and Infrastructure Management, Ministry of Land, Infrastructure and Transport, Japan. [In Japanese.]

Savage, S. B., and Hutter, K. 1989. “The motion of a finite mass of granular material down a rough incline.” *Journal of fluid mechanics 199*, 177–215. https://doi.org/10.1017/S0022112089000340.

Song, D., Ng, C.W.W., Choi, C.E., Zhou, G.G.D., Kwan, J.S.H., and Koo, R.C.H. 2017. “Influence of debris flow solid fraction on rigid barrier impact.” *Can. Geotech. J.* 54(12): 1421-1434. https://doi.org/10.1139/cgj-2016-0502.

Song, D., Choi, C.E., Zhou, G.G.D., Kwan, J.S.H., and Sze, H.Y. 2018. “Impulse load

characteristics of bouldery debris flow impact." *Géotechnique Letters* 8(2): 111–117. https://doi.org/10.1680/jgele.17.00159.
Song, D., Choi, C. E., Ng, C. W. W., Zhou, G. G., Kwan, J. S., Sze, H. Y., and Zheng, Y. 2019. "Load-attenuation mechanisms of flexible barrier subjected to bouldery debris flow impact." *Landslides* https://doi.org/10.1007/s10346-019-01243-2.
Sovilla, B., Faun, T., Köhler, A., Baroudi, D., Fischer, J. T., and Thibert, E. 2016. "Gravitational wet avalanche pressure on pylon-like structures." *Cold Regions Sci. Technol.* 126,66–75. https://doi.org/10.1016/j.coldregions.2016.03.002.
Su, Y., Cui, Y, Ng, C.W.W, Choi, C. E., and Kwan, J.S.H. 2019. "Effects of particle size and cushioning thickness on the performance of rock-filled gabions used in protection against boulder impact." *Can. Geotech. J.* 56(2): 198–207. https://doi.org/10.1139/cgj-2017-0370.
Sun, H.W., Lam, T.T.M., and Tsui, H.M. 2005. *Design basis for standardised modules of landslide debris-resisting barriers.* GEO Report No. 174. Geotechnical Engineering Office, Civil Engineering and Development Department, The HKSAR Government.
SWCB. 2005. *Manual of soil and water conservation.* Soil and Water Conservation Bureau, Taiwan. [In Chinese.]
Vagnon, F., and Segalini, A. 2016. "Debris flow impact estimation on a rigid barrier." *Nat. Hazards Earth Syst. Sci. 16*(7): 1691–1697. https://doi.org/10.5194/nhess-16-1691-2016.
VanDine, D.F. 1996. *Debris Flow Control Structures for Forest Engineering*. Ministry of Forests, British Columbia, Canada, 68 p.
Volkwein, A. 2014. *Flexible debris flow barriers: Design and application.* WSL Berichte, 18. Birmensdorf, Swiss Federal Institute for Forest, Snow and Landscape Research WSL. 29 p.
Wang, H., Yin, X., Hao, H., Chen, W. and Yu, B. 2020. "The correlation of theoretical contact models for normal elastic-plastic impacts." *Int. J. Solids Struct.* 182:15–33. https://doi.org/10.1016/j.ijsolstr.2019.07.018.
Wendeler, C, and Volkwein, A. 2015. "Laboratory tests for the optimization of mesh size for flexible debris-flow barriers." *Nat. Hazards Earth Syst. Sci.* 15: 2597–2604. https://doi.org/10.5194/nhess-15-2597-2015.
Wendeler, C., Volkwein, A., McArdell, B. W., and Bartelt, P., 2019. "Load model for designing flexible steel barriers for debris flow mitigation." *Can. Geotech. J. 56*(6): 893-910. https://doi.org/10.1139/cgj-2016-0157.
Yigit, A.S., Christoforou, A.P., and Majeed, M.A. 2011. "A nonlinear visco-elastoplastic impact model and the coefficient of restitution." *Nonlinear Dynamics 66*(4): 509–521. https://doi.org/10.1007/s11071-010-9929-6.
Zeng, C., Cui, P., Su, Z., Lei, Y., and Chen, R. 2015. "Failure modes of reinforced concrete columns of buildings under debris flow impact." *Landslides* 12(3): 561–571. https://doi.org/10.1007/s10346-014-0490-0.
Zhang, S. 1993. "A comprehensive approach to the observation and prevention of debris flows in China." *Natural Hazards* 7(1): 1–23. https://doi.org/10.1007/BF00595676.
Zhang, L.M., Xu, Y., Huang, R.Q., and Chang, D.S. 2011. "Particle flow and segregation in a giant landslide event triggered by the 2008 Wenchuan earthquake, Sichuan, China." *Nat. Hazards Earth Syst. Sci.* 11(4): 1153–1162. http://doi.org/10.5194/nhess-11-1153-2011.
Zhou, G.G.D., Song, D., Choi, C.E., Pasuto, A., Sun, Q.C., and Dai, D.F. 2018. "Surge impact of granular flows: effects of water content." *Landslides* 15(4): 695–709. https://doi.org/10.1007/s10346-017-0908-6.
Zhou, G.G.D., Du, J., Song, D., Choi, C.E., Hu, H.S., and Jiang, C. 2019. "Numerical study on granular debris flow runup against slit-dams by discrete element method." *Landslides* https://doi.org/10.1007/s10346-019-01287-4.

Table 1. Test programme and results

Test ID	Debris volume (m^3)	Quantity of boulders	Initial debris density (kg/m^3)	Debris frontal velocity, v (m/s)	First boulder velocity, v_b (m/s)	Flow depth, h (mm)	Froude number, Fr	Peak impact force (kN)	K_c
D	2.5	0	1960	5.2	—	50	7.4	4.9	—
DB10	2.5	10	1960	5.5	7.5	50	7.9	27.1	0.04
B1	0	1	—	—	6.0	—	—	41.3	0.08
B10	0	10	—	—	7.1	—	—	71.5	0.11

Table 2. Debris composition

Material	Average diameter (mm)	Bulk density (kg/m^3)	Mass fraction by total weight (%)	Mass fraction by dry weight (%)	Volume percentage (%)
Gravel	20	558	28	36	21
Sand	2	957	49	61	36
Clay	<0.006	43	2	3	2
Water	—	344	21	—	41
Total	—	1960	100	100	100

Fig. 1

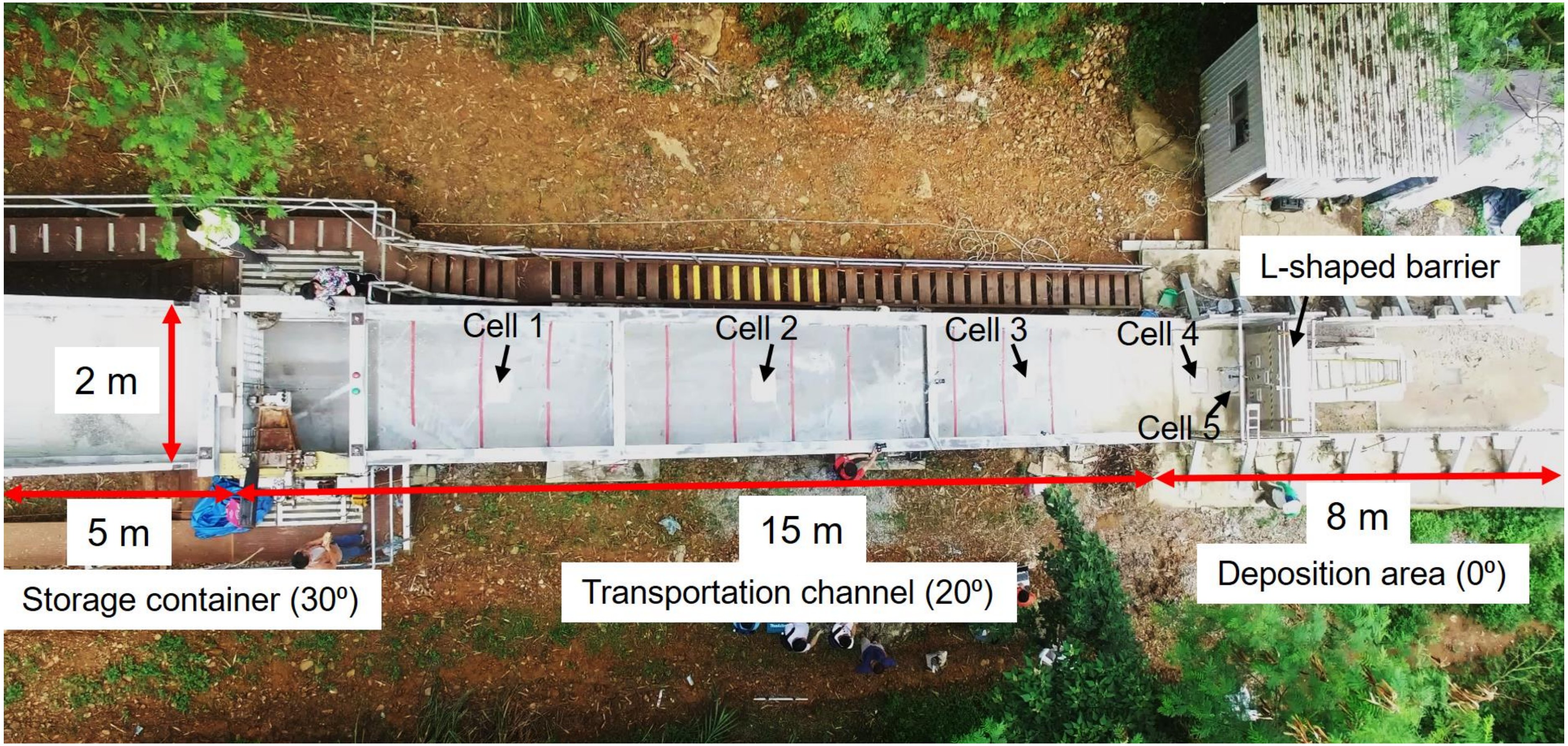

L-shaped barrier
Cell 1
Cell 2
Cell 3
Cell 4
Cell 5
2 m
5 m
15 m
8 m
Storage container (30º)
Transportation channel (20º)
Deposition area (0º)

Fig. 2

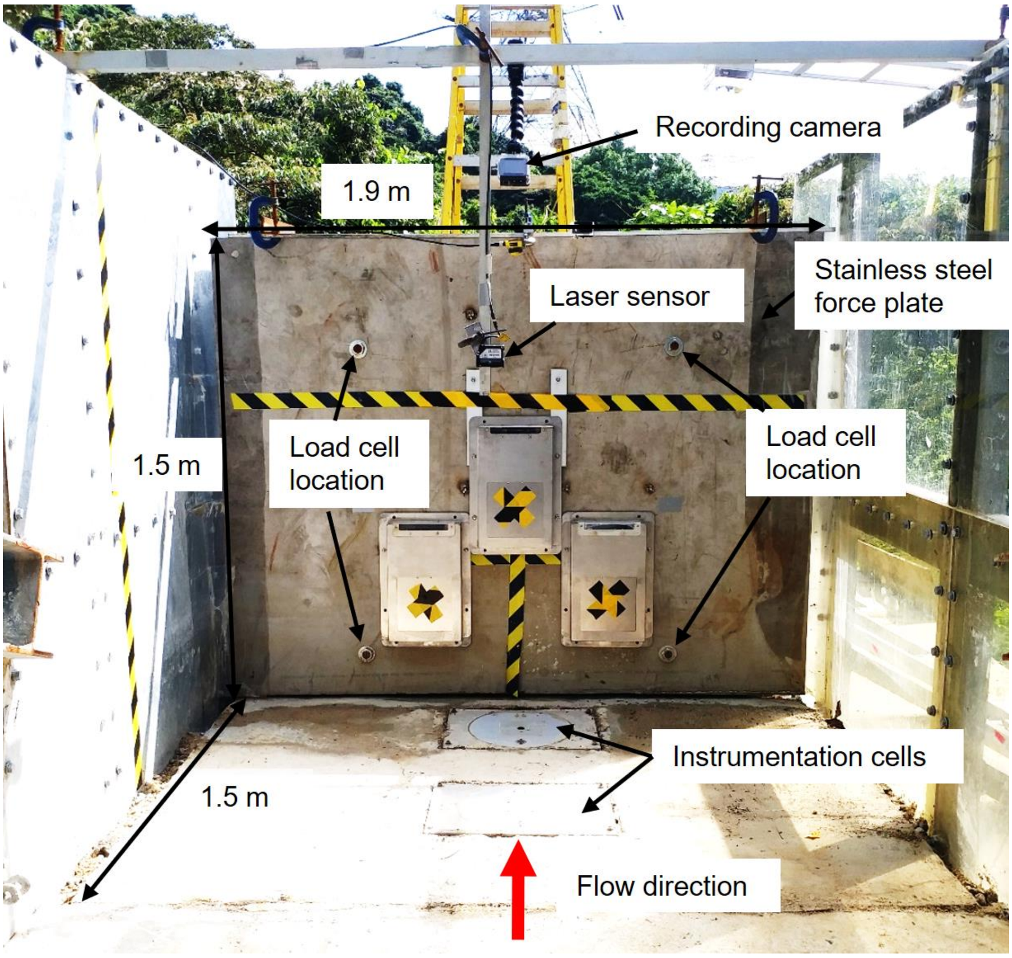
Recording camera
1.9 m
Laser sensor
Stainless steel
force plate
Load cell
location
Load cell
location
1.5 m
Instrumentation cells
1.5 m
Flow direction

Fig. 3

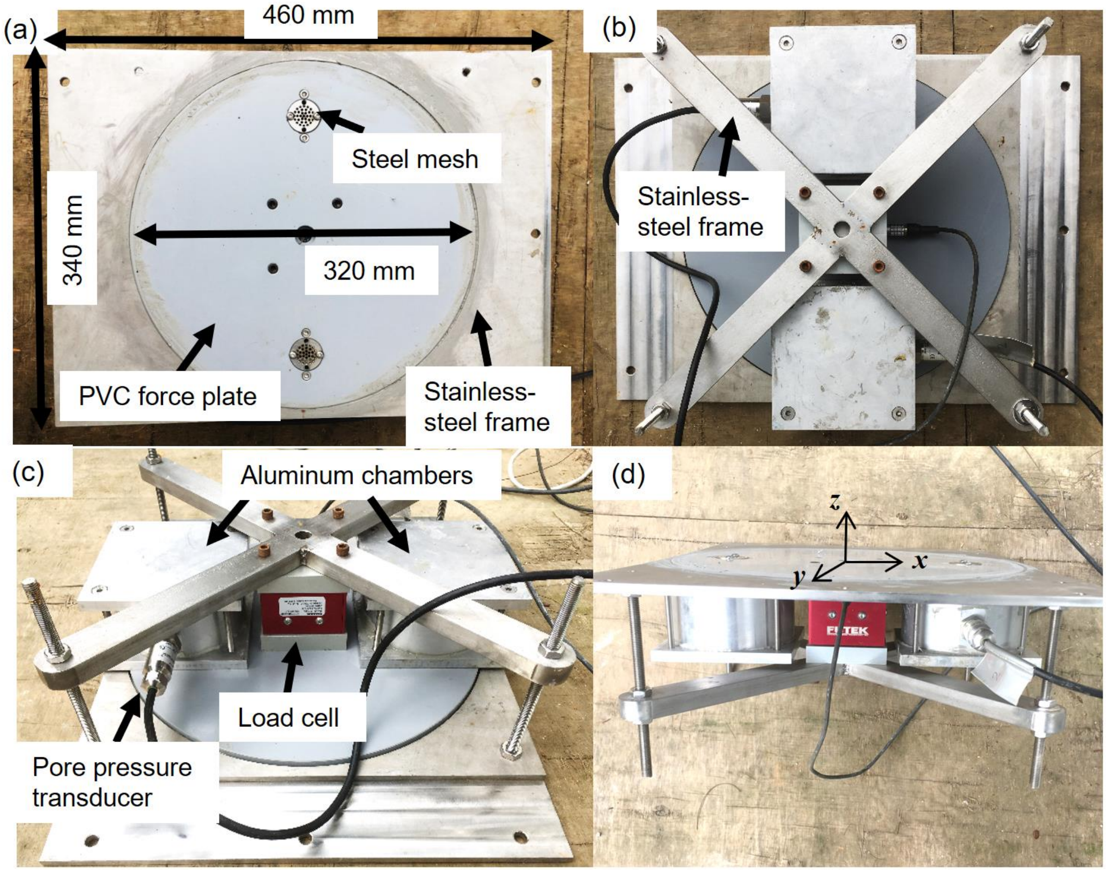
(a)
460 mm
340 mm
Steel mesh
320 mm
PVC force plate
Stainless-steel frame
(b)
Stainless-steel frame
(c)
Aluminum chambers
Load cell
Pore pressure transducer
(d)
z
x
y

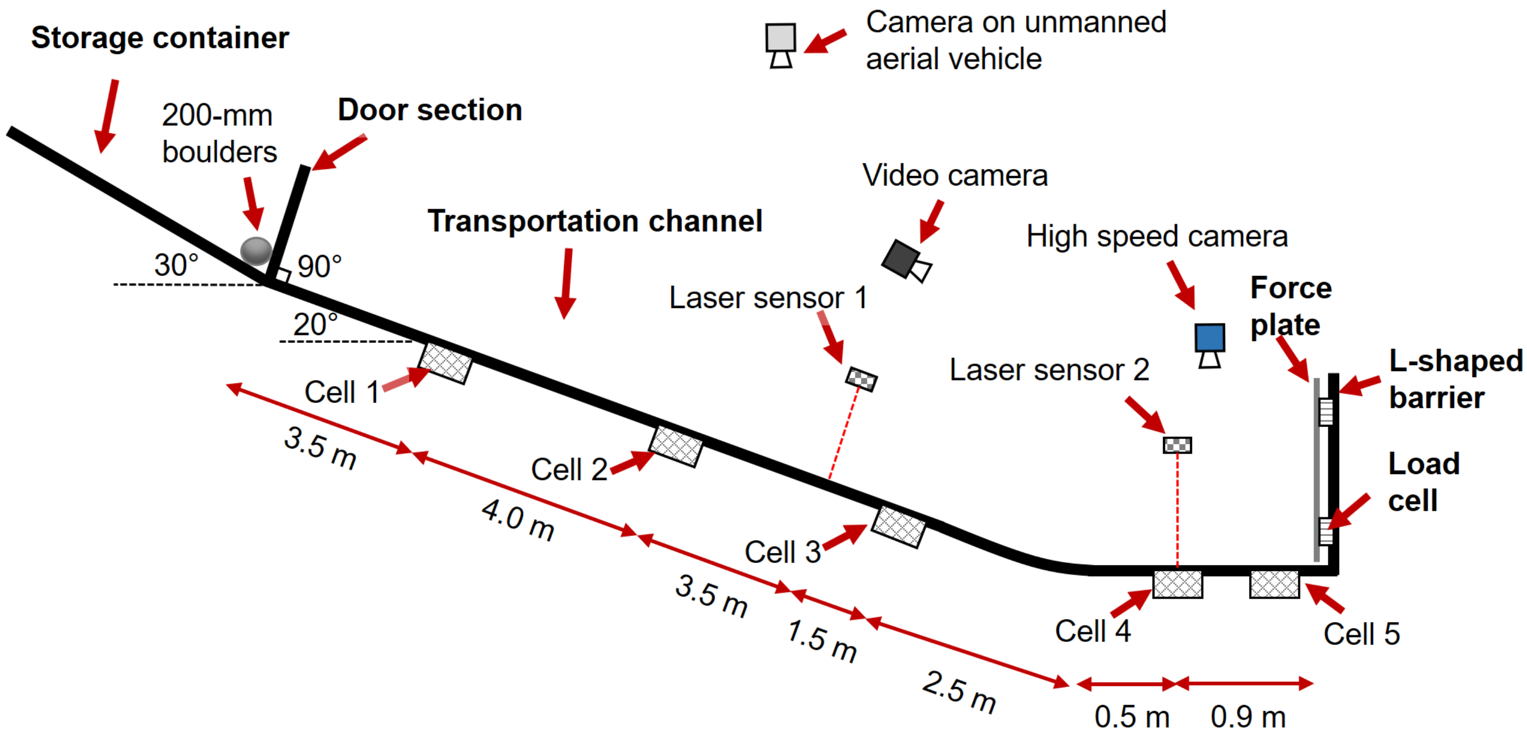
Storage container
200-mm
boulders
Door section
Camera on unmanned
aerial vehicle
Video camera
Transportation channel
High speed camera
Laser sensor 1
Force
plate
L-shaped
barrier
Laser sensor 2
Load
cell
30°
90°
20°
Cell 1
Cell 2
Cell 3
Cell 4
Cell 5
3.5 m
4.0 m
3.5 m
1.5 m
2.5 m
0.5 m
0.9 m

Fig. 5

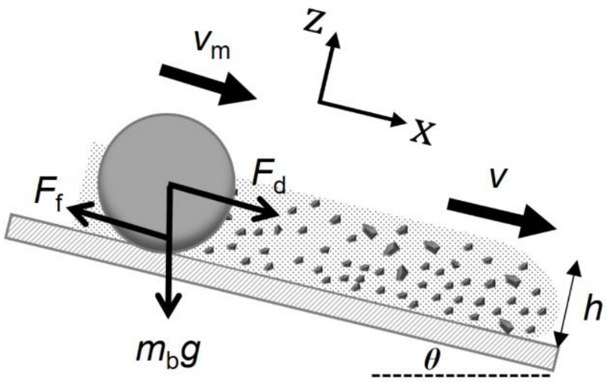

Fig. 6

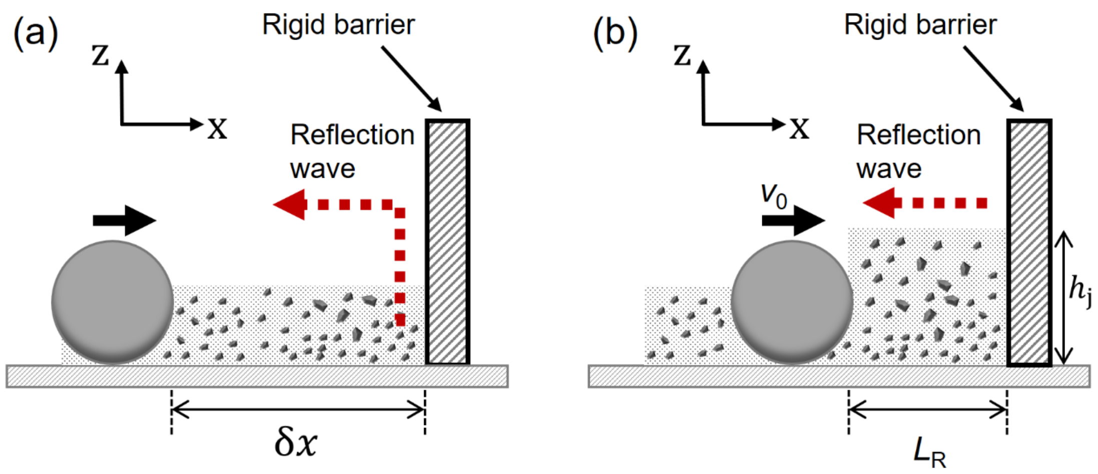
(a)
Rigid barrier
z
x
Reflection wave
δx
(b)
Rigid barrier
z
x
Reflection wave
v0
hj
LR

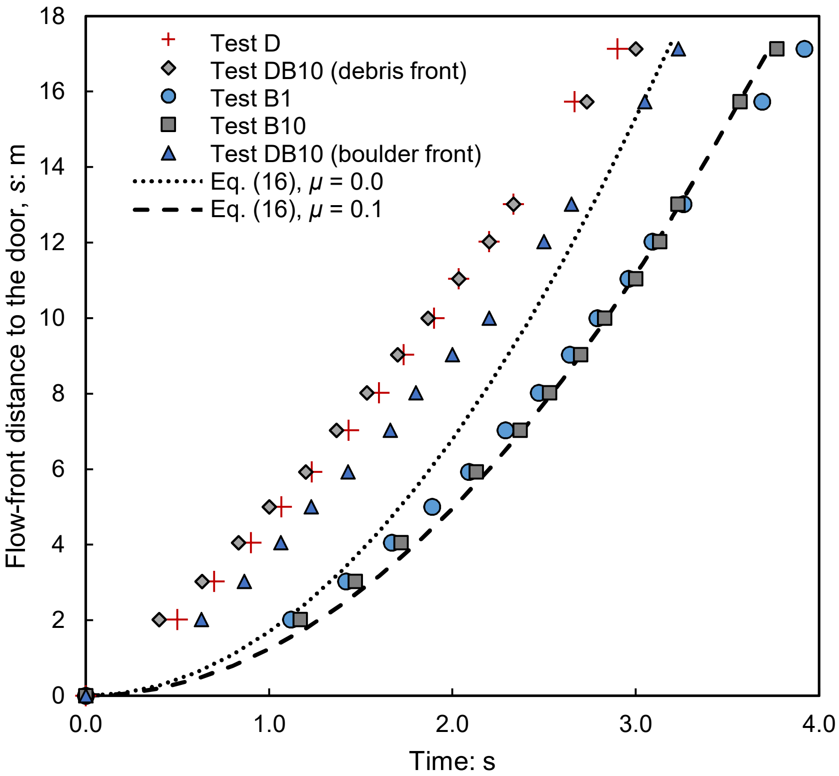
Test D
Test DB10 (debris front)
Test B1
Test B10
Test DB10 (boulder front)
Eq. (16), μ = 0.0
Eq. (16), μ = 0.1
Flow-front distance to the door, s: m
Time: s
0
2
4
6
8
10
12
14
16
18
0.0
1.0
2.0
3.0
4.0

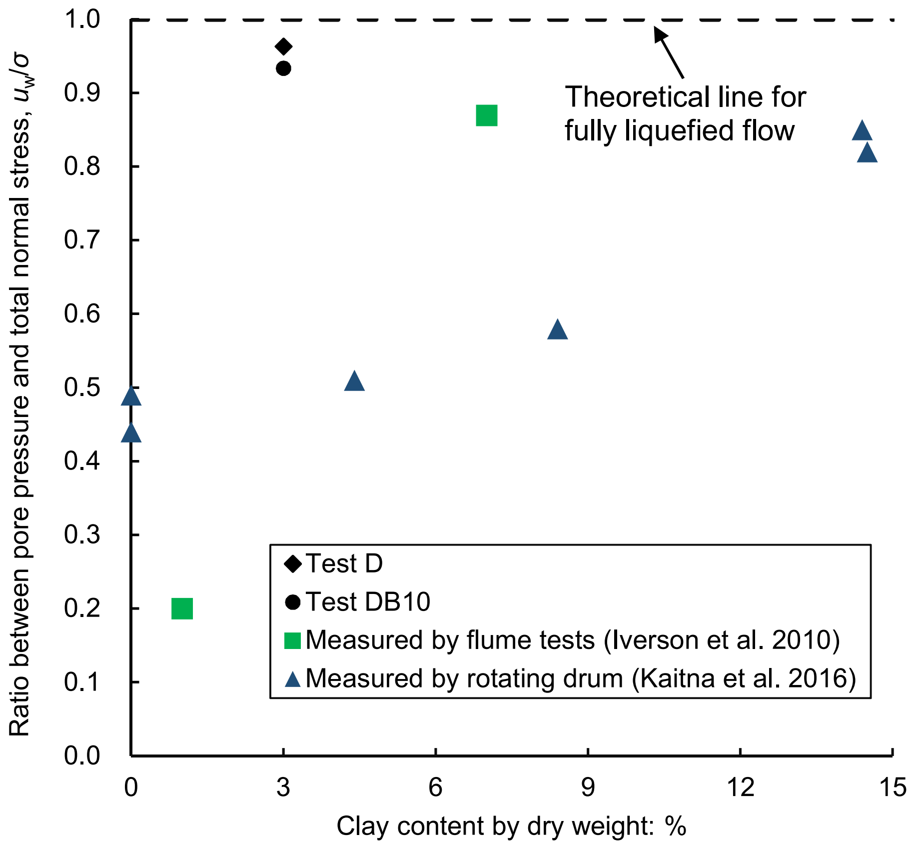
Ratio between pore pressure and total normal stress, u_w/σ
1.0
0.9
0.8
0.7
0.6
0.5
0.4
0.3
0.2
0.1
0.0
0
3
6
9
12
15
Clay content by dry weight: %
Theoretical line for
fully liquefied flow
Test D
Test DB10
Measured by flume tests (Iverson et al. 2010)
Measured by rotating drum (Kaitna et al. 2016)

Fig. 9

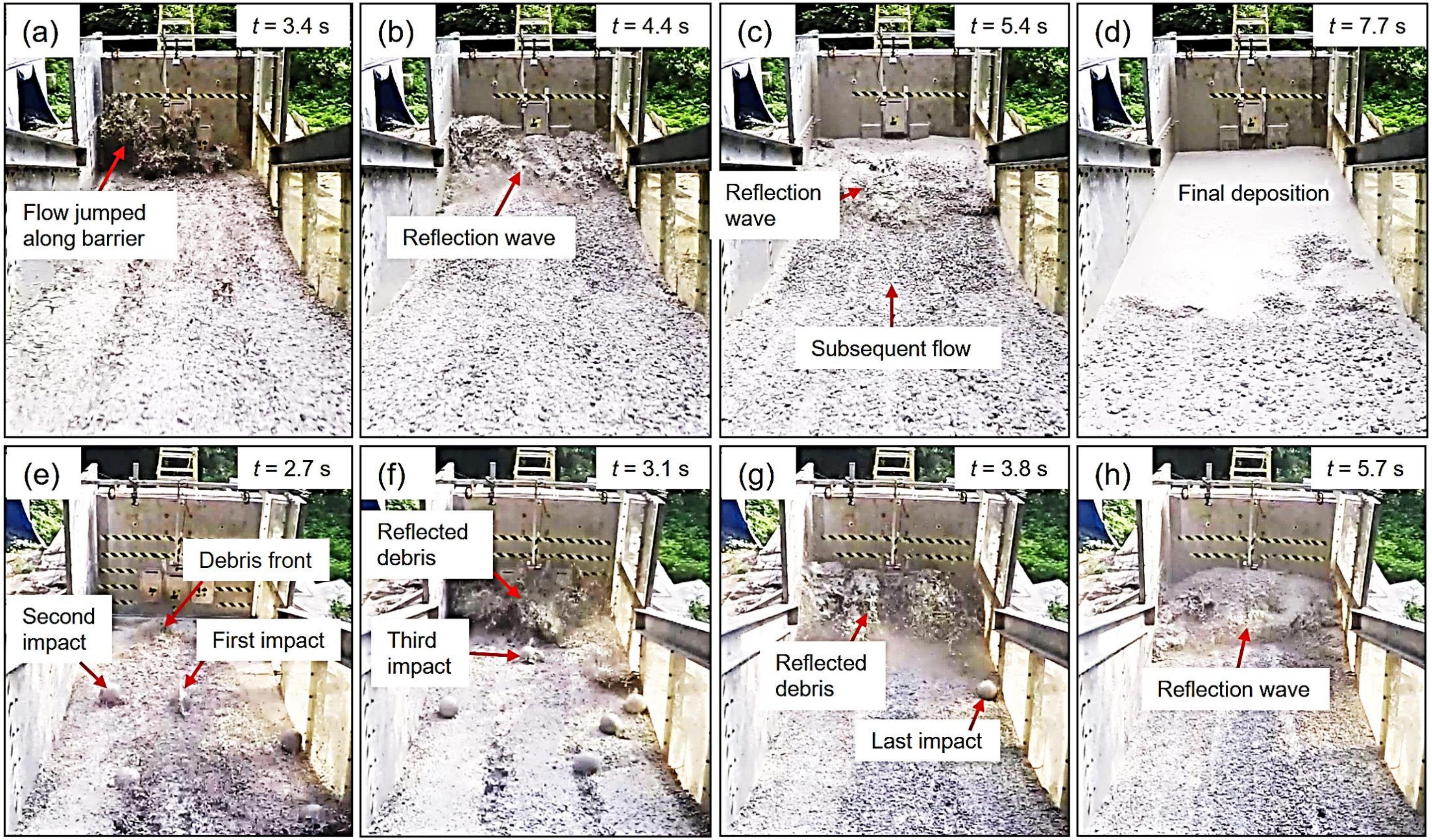
(a)
t = 3.4 s
Flow jumped along barrier
(b)
t = 4.4 s
Reflection wave
(c)
t = 5.4 s
Reflection wave
Subsequent flow
(d)
t = 7.7 s
Final deposition
(e)
t = 2.7 s
Debris front
Second impact
First impact
(f)
t = 3.1 s
Reflected debris
Third impact
(g)
t = 3.8 s
Reflected debris
Last impact
(h)
t = 5.7 s
Reflection wave

Fig. 10

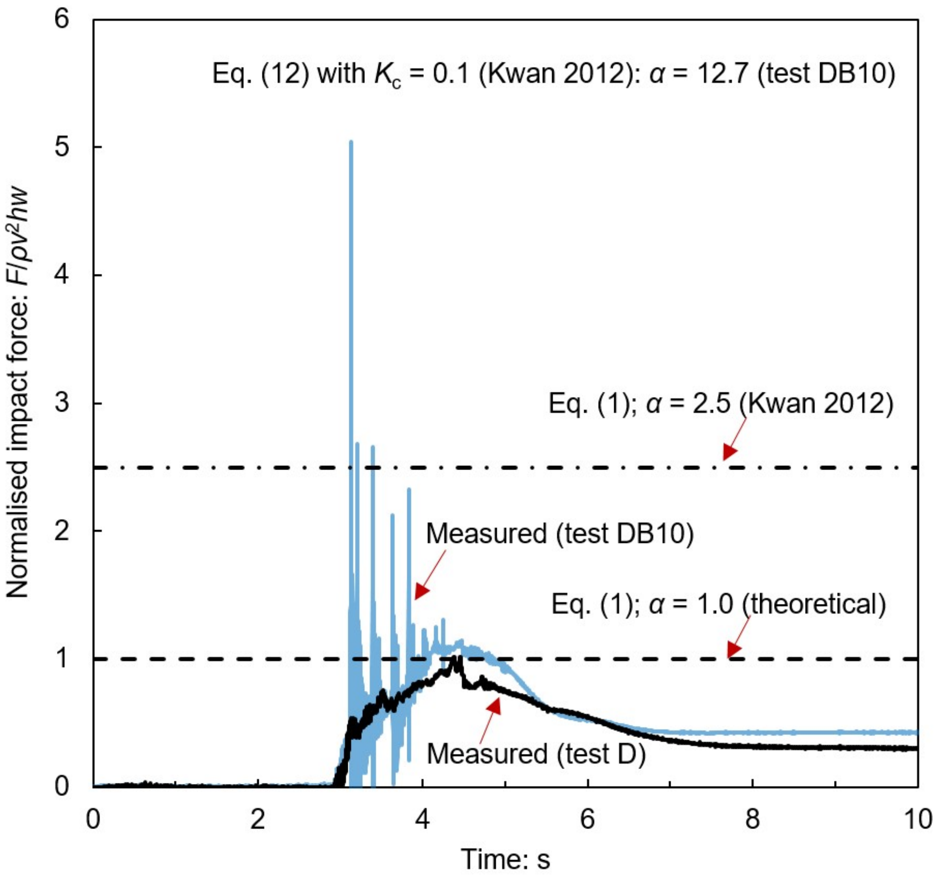

Eq. (12) with K_c = 0.1 (Kwan 2012): α = 12.7 (test DB10)
Eq. (1); α = 2.5 (Kwan 2012)
Measured (test DB10)
Eq. (1); α = 1.0 (theoretical)
Measured (test D)
Normalised impact force: $F/\rho v^2 hw$
Time: s
0
1
2
3
4
5
6
0
2
4
6
8
10

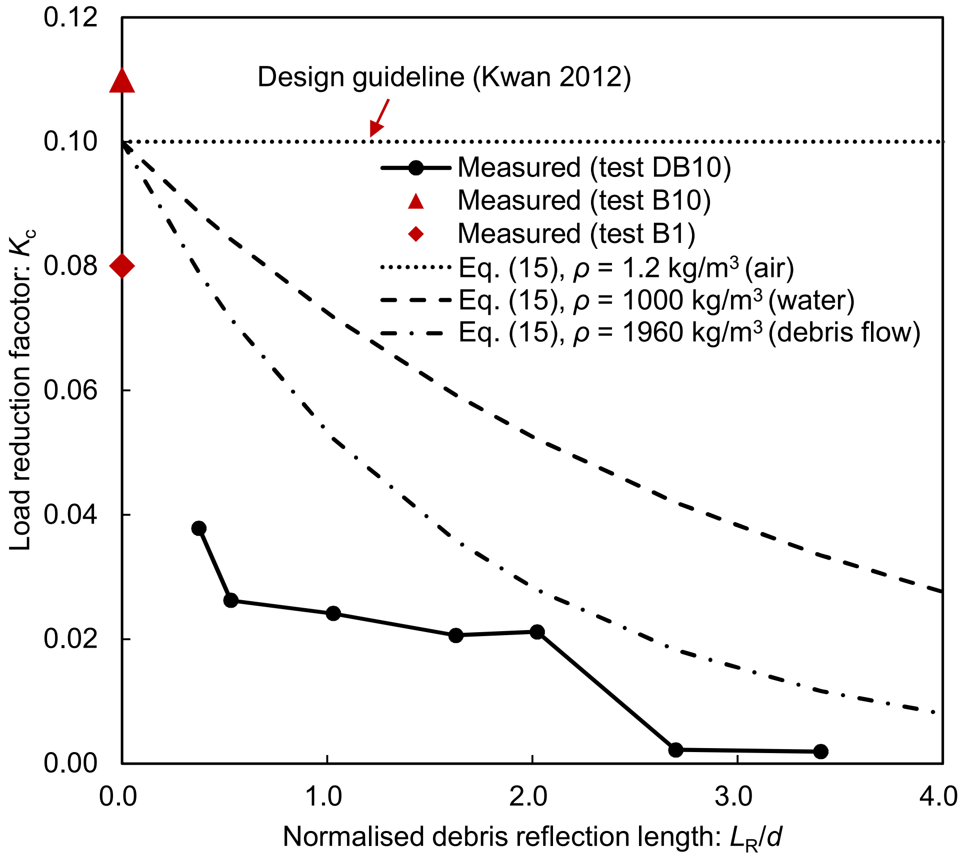
0.12
0.10
0.08
0.06
0.04
0.02
0.00
Load reduction facotor: K_c
Design guideline (Kwan 2012)
Measured (test DB10)
Measured (test B10)
Measured (test B1)
Eq. (15), ρ = 1.2 kg/m^3 (air)
Eq. (15), ρ = 1000 kg/m^3 (water)
Eq. (15), ρ = 1960 kg/m^3 (debris flow)
0.0
1.0
2.0
3.0
4.0
Normalised debris reflection length: L_R/d

List of Figure Captions

Fig. 1. Plan view of the flume facility.

Fig. 2. Front view of the L-shaped reinforced concrete barrier.

Fig. 3. Details of the instrumentation cell: (a) top view; (b) bottom view; (c) bottom side view; (d) top side view.

Fig. 4. Side schematic of the test and instrumentation setup (not drawn to scale).

Fig. 5. Side schematic of the boulder motion in a debris flow.

Fig. 6. Side schematic of the boulder motion during debris flow impact: (a) debris front just reaches barrier location; (b) boulder starts to interact with the debris reflection wave.

Fig. 7. Time histories of frontal position of boulders and debris flow.

Fig. 8. Measured liquefaction ratio at different clay contents.

Fig. 9. Observed impact kinematics of debris flow (test D): (a) to (d), and debris flow with ten boulders (test DB10): (e) to (h).

Fig. 10. Time histories of the normalised impact force of debris flow (test D) and debris flow with ten boulders (test DB10).

Fig. 11. Comparison of load reduction factor against normalised debris reflection length.

July 9, 2020

Manuscript No. GTENG-8770

Reply to Comments from Editor and Reviewers

(C and R denote comment and reply, respectively)

Editor

C1: Thank you for your submission to the Journal of Geotechnical and Geoenvironmental Engineering. Two reviewers have provided constructive feedback below that can help strengthen your manuscript.

I have also reviewed your manuscript with great interest. The experimental setup is impressive and the results and conclusions are valuable to practice. One caveat that is mentioned in the text but I think should be emphasized in the conclusions is the range of debris flow materials over which your results are valid. Because of the high variability that has been observed in debris flow materials it is important to clearly define the bounds of your study in the concluding remarks.

R1: As instructed, we have now clearly stated the debris flow composition over which our results are valid in the conclusions **(*Page 22; Lines 490 to 494*)**.

> *"The results from this study were based on a debris flow mixture of gravel, sand, clay and water with volumetric fractions of 0.21, 0.36, 0.02 and 0.41, respectively. The gravel and sand had average sizes of 20 mm and 2 mm, respectively. The clay had a particle size smaller than 0.006 mm. Boulders adopted by this study were spherical granite with a uniform diameter of 200 mm."*

C2: Based on the reviewer feedback and my own review the decision is that the manuscript should be Revised for Re-review before it can proceed to publication. To proceed please provide a point-by-point response to each review comment, and provide a marked copy with edits to aid in the re-review process. Once revised your manuscript will be returned to the same reviewers for a second assessment. Please contact me if you have any questions.

R2: Thank you for the positive feedback. We have now carefully addressed the comments from each reviewer and provided a detailed response below.

Reviewer 1

C1: The authors conducted experiments to analyze the impact load on a barrier by debris flows with and without boulders. A new equation is also proposed to interpret the experimental results. The study may be useful to evaluate geo-hazards such as mudslides.

R1: Thank you for your positive and helpful comments. We have now carefully addressed each of your comments in detail below.

C2: An equation is derived to estimate the impact load with debris cushions in this study. The derivation is based on elastic Hertz contact. However, plastic deformation may exist for the impact between a boulder and a barrier as the authors mentioned. An empirical coefficient is introduced to consider the plastic deformation. Please check whether better methods are available to consider the plastic deformation in the literature.

R2: Thank you for your valuable comment. We have now carefully reviewed other impact models in the literature that explicitly consider plastic deformation and added this useful information to our manuscript. Based on our literature review, it appears that the Hertz model together with an empirical coefficient is the most commonly adopted approach in engineering design practice. The empirical coefficient in the hertz equation implicitly considers plastic deformation (SWCB 2005; NILIM 2007; Kwan 2012). We have now included more discussion in the revised manuscript **(*Pages 19 to 20; Lines 433 to 446*)**:

> *"In this study, the Hertz model together with an empirical coefficient that implicitly considers plastic deformation was adopted to estimate the boulder impact force. It is worthwhile to mention that there are also analytical models that can explicitly consider the plastic deformation during boulder impact (Yigit et al. 2011; Brake 2012; Ma and Liu 2015). These methods usually require information on the evolution of the plastic regions (Ma and Liu 2015). However, difficulty in measuring such data has hindered a well-accepted approach that considers plastic deformation. Wang et al. (2020) summarised 18 theoretical elastoplastic contact models and found that the definition of the yield condition during loading phase is necessary for an accurate prediction of the impact. Evidently, a further investigation of the yield criterion for boulder impact on barriers would enhance a more rational approach for estimating boulder impact force. Nevertheless, the more pragmatic engineering approach with an empirical coefficient K_c as expressed in Eqs. (2) ~ (6) has the merit of being simple and robust enough for*

> *engineering design and is currently widely adopted in engineering practice internationally (SWCB 2005; NILIM 2007; Kwan 2012).”*

Eqs. (2) ~ (6) are shown as follows for an easy reference:

$$F_\mathrm{b} = K_\mathrm{c} n a^{1.5} \tag{2}$$

$$n = \frac{4r_\mathrm{b}^{0.5}}{3\pi(k_\mathrm{b} + k_\mathrm{B})} \tag{3}$$

$$a = \left(\frac{5m_\mathrm{b}v_\mathrm{b}^2}{4n}\right)^{0.4} \tag{4}$$

$$k_\mathrm{b} = \frac{1-\mu_\mathrm{b}^2}{\pi E_\mathrm{b}} \tag{5}$$

$$k_\mathrm{B} = \frac{1-\mu_\mathrm{B}^2}{\pi E_\mathrm{B}} \tag{6}$$

C3: 2. Different numbers of boulder are considered in the experiments. Please further explain whether and how this aspect is considered in the proposed equation.

R3: Thank you for your pertinent comment. The proposed equation in this study cannot consider the effects of different numbers of boulder on the load reduction factor K_c. We have now stressed this as a limitation of our approach and supplemented explanation about the potential effects of different numbers of boulder in the manuscript as follows ***(Page 19; Lines 425 to 432)***:

> *“The proposed Eq. (15) does not consider the effects of the number of boulders on load reduction factor K_c. In this study, the performance of the Eq. (15) is only verified by debris flow that entrained ten spherical boulders with a boulder fraction of up to 2% of the debris flow volume. For debris flows with a much larger number of boulders and a much higher boulder fraction, the frictional and collisional stresses among boulders may be more prominent than the damping provided by the debris flow. Therefore, the proposed equation may be required to be modified for a much higher boulder fraction. A further investigation of the effects of boulder fractions on the impact dynamics of boulder-enriched debris flow is still warranted.”*

Eq. (15) is shown as follows for reference:

$$K_c = 0.1e^{-0.9C_d\frac{\rho L_R}{\rho_b d}} \quad (15)$$

C4: 3. This study introduced a dimensionless parameter L_R/d to consider the cushioning effect. But only one value of the diameter is considered in the experiments. It would be better if different values of L_R, d, and L_R/d were considered. The proposed dimensionless parameter L_R/d approaches a large number when the diameter d is very small.

R4: Thank you for your valuable comment. Given the restrictions in terms of cost and time for large-scale flume tests, only one boulder diameter was adopted in our experimental campaign. We have now included more discussion in our revised manuscript about our limitation and we have now recommended that the proposed Eq. (15) should be adopted only when the diameter of the boulder is larger than 0.6 times of the flow depth and smaller than the thickness of the reflection wave. Also, we have now clearly provided the physical meaning when L_R/d approaches to 0 and infinity. ***(Pages 18 to 19; Lines 406 to 424)***

> *"It should be noted that spherical boulders with a uniform diameter were adopted in this study to easily characterise boulder kinematics and dynamics without the influence of different boulder sizes and shapes. The proposed Eq. (15) assumes that the diameter of the boulder d is smaller than the thickness of the reflection wave h_j as shown in Fig. 6b. It is expected that the proposed Eq. (15) holds for boulders with a diameter $d < h_j$ because this diameter is consistent with the assumptions made by Eq. (15). Song et al. (2018) recommended that Eqs. (2) ~ (6) should be adopted to estimate the boulder impact force for boulders that have a diameter larger than 0.6 times of the flow depth h. Therefore, boulder with a diameter $0.6h < d < h_j$ is recommended for adopting Eq. (15). For a small boulder that has a size approaching 0, the L_R/d approaches infinity, the cushioning effect of the reflected debris on the boulder is very significant and boulder impact force can be neglected. For this condition, K_c equals to 0 as calculated by Eq. (15). The impact force of the debris flow can be calculated by only using the continuum approach, such as the hydrodynamic equation [Eq. (1)]. For boulder that has a diameter larger than h_j, the effects of viscous damping may be reduced due to the smaller contact area compared with the area that a boulder is fully immersed in the flow. Notwithstanding, a $K_c = 0.1$ would still be adopted to provide a conservative prediction. When $d \gg L_R$ and L_R/d approaches 0, the cushioning effect from the reflected debris can be neglected due to the negligible cushioning thickness and K_c should be taken as 0.1 to estimate the boulder impact force in a debris flow."*

Fig. 6b is shown as follows for reference:

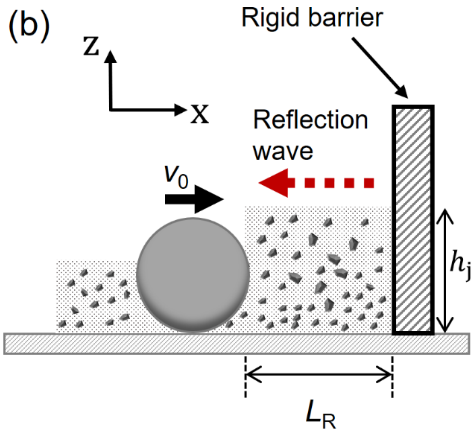

Fig. 6b. Side schematic of the boulder motion during debris flow impact: boulder starts to interact with the debris reflection wave.

C5: 4. Please further explain the difference between Eq. 16 and experiment data in Fig. 7.

R5: As instructed, we have now further explained the difference between Eq. (16) and our measurements in Fig. 7 in ***Pages 11 to 12; Lines 238 to 248***:

> *"The flow distance for a frictionless point mass (μ = 0.0) calculated by Eq. (16) is shown in Fig. 7. The time history of this flow distance underestimates the measured motion of debris fronts for both debris flow test (test D) and the test of debris flow with ten boulders (test DB10). The underestimation may be attributed to the larger longitudinal pressure compared with the basal friction as expressed in Eq. (17). This caused a larger acceleration than the acceleration of a frictionless point mass* $g \sin\theta$*. Eq. (16) with μ = 0.0 overestimates the motion of boulder front when there is no debris flow but underestimates the motion of boulder front when boulders are entrained in debris flow. The overestimation may be mainly caused by the deceleration of the boulder motion due to basal friction. The underestimation may be mainly attributed to the acceleration of the boulder motion due to the drag force from debris flow as expressed in Eq. (11)."*

Eqs. (11), (16) and (17) and Fig. 7 are shown as follows for reference:

$$\frac{dv_m}{dt} = g\,sin\,\theta - \mu g\,cos\,\theta + \frac{C_d A \rho \delta v^2}{2m_b} \tag{11}$$

$$s = \frac{g \sin\theta - \mu g \cos\theta}{2} t^2 \tag{16}$$

$$\frac{du}{dt} = g \sin\theta - \mu g \cos\theta - k\frac{\partial h}{\partial x} g \cos\theta \tag{17}$$

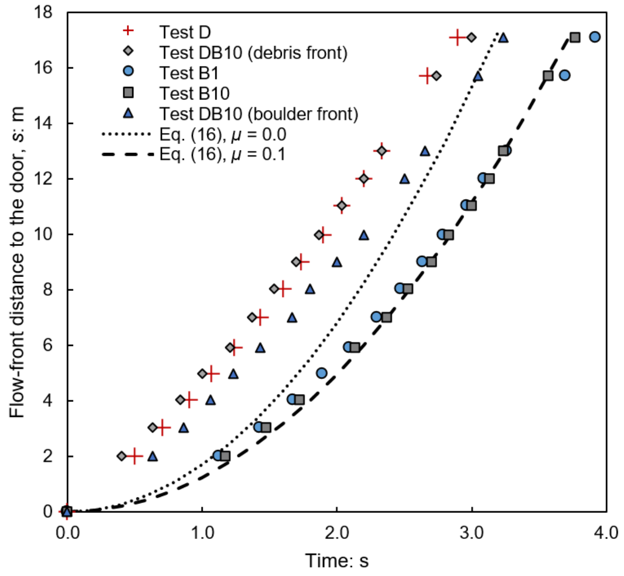

Fig. 7. Time histories of frontal position of boulders and debris flow.

Other minor comments:

C6: 1. Please remove commercial related information, such as "GoPro HERO5" and "DJI Phantom 3 Standard."

R6: As instructed, we have now removed all the commercial related information of our test equipment throughout the manuscript. However, we wish to point out that reviewer #2 has suggested us to include a discussion on current software. Therefore, we have remained some information about commercial software.

C7: 2. Put the coefficient 6100 in front of Kc in Eq. 12.

R7: Thank you for your comment. The correction has now been made.

Reviewer 2

C1: It is an interesting article with practical applications. The authors present a theoretical framework and experimental studies to correlate their findings. My only concern is regarding the practical application. Debris flows barriers around the world are generally designed with conservative assumptions as indicated by the manuscript, however the level of uncertainty on factors such as material gradation makes it very difficult to refine the analysis. Moreover, the available commercial software tends to approximate conditions so analyses can be performed. In this respect being conservative is a good thing given the level of risk. The authors should include a discussion on current software and products (flexible vs rigid; closed vs open barriers; attenuators vs actual barriers, etc) that are actually used in practice. It is the experience of the reviewer that a fully "experimental" and "conservative" approach is used these days because of the given uncertainty of the debris flow composition. Perhaps the findings of these study can help on bringing some attention to a more appropriate way of modeling without compromising safety.

R1: Thank you for your positive and constructive comment. We have now included a new section with a title of "***Implications for designing debris-resisting barriers in practice***" to discuss the practical application from this study and current software packages and types of barriers adopted in practice **(*Pages 20 to 21; Lines 447 to 487*)**.

> *"The impact dynamics of debris flow against debris-resisting barriers are not well understood because of the heterogeneous nature of debris flows and the idiosyncrasies of the natural settings involved. Therefore, to ensure a conservative barrier design, the above-mentioned factors should be considered. To highlight the general dearth of knowledge in estimating boulder impact, an empirical load reduction factor of 0.1 is required to reduce the impact load predicted using the elastic Hertz equation [Eq. (12)]. Kwan (2012) suggested that if simultaneous boulder impact may occur, the design impact load per meter run of the barrier should be taken as the impact load of the largest boulder divided by the boulder diameter. Following this approach, the total design impact load for the rigid barrier is 650 kN, which is 23 times higher than the measured peak impact load for debris flow with ten boulders from the physical experiments in this study (Fig. 10; test DB10). Evidently, there is room to enhance our understanding and to optimise the current design load of boulder-enriched debris flows.*
>
> *Aside from the complexities attributed to the debris flow itself and the natural terrain, different types of debris-resisting barriers may also result in entirely different impact processes and dynamics. The results in this study are for a fully closed rigid barrier without overflow or barrier deformation. For open structures,*

such as baffles (Choi et al. 2015; Law et al. 2015; Ng et al. 2015) and slit dams (Choi et al. 2016; Zhou et al. 2019), debris may discharge through and around these structures and the cushioning effect identified in this study may not be as prominent as compared with that for closed barriers. For flexible barriers (Wendeler and Volkwein 2015; Wendeler et al. 2019; Song et al. 2019), the deformation of the barrier may lead to a different debris reflection compared with rigid barriers and alter the boulder-flow-barrier interaction process. To further rationalise the design of debris-resisting barriers in practice, advanced numerical modelling methods together with high quality physical data can potentially optimise the resisting capacity required by a barrier.

In engineering design practice, well calibrated numerical models are utilised to optimise designs. For instance, a depth-averaged continuum numerical software 2d-DMM (Kwan and Sun 2006; Law and Ko 2018) and a finite element software package LS-DYNA (Crosta et al. 2003) have been recommended by design guidelines (Kwan 2012; Koo 2017) to obtain the design velocity and flow depth to estimate impact loads. Koo (2017) also recommended the use of LS-DYNA to model the impact dynamics of flow against rigid (Ng et al. 2018) and flexible (Koo and Kwan 2014; Cheung et al. 2018) barriers. Although LS-DYNA can also model boulder impact (Koo and Kwan 2014; Ng et al. 2018), a deficiency of unique reliable large-scale data has hindered model calibration. The findings from this study stress the importance of modelling the debris and boulder separately for the design of barriers. More recently, coupled approaches using the discrete element method with computational fluid dynamics have been reported (Li and Zhao 2018). However, the computational cost for such an approach limits its use for larger scale problems in practical engineering design. The observed importance of capturing the boulder and debris loads separately in this study further suggests that more advanced numerical approaches are needed to advance the state-of-the-art and rationalise the design of debris-resisting barriers."

Additional references:

Brake, M. 2012. "An analytical elastic-perfectly plastic contact model." *Int. J. Solids Struct.* 49(22): 3129–3141. https://doi.org/10.1016/j.ijsolstr.2012.06.013.

Cheung, A.K.C, Yiu, J., Lam, H.W.K, and Sze, E.H.Y. 2018. "Advanced numerical analysis of landslide debris mobility and barrier interaction." *HKIE Transactions* 25(2):76–89. https://doi.org/10.1080/1023697X.2018.1462106.

Crosta, G.B., Imposimato, S., and Roddeman, D.G. 2003. "Numerical modelling of large landslides stability and runout." *Natural Hazards and Earth System Sciences* 3:523–538. https://doi.org/10.5194/nhess-3-523-2003.

Koo, R.C.H. 2017. *3D debris mobility assessment using LS-DYNA.* GEO Report No. 325. Geotechnical Engineering Office, Civil Engineering and Development Department, The HKSAR Government.

Koo, R.C.H., and Kwan, J.S.H. 2014. *A Numerical study of dynamic responses of two selected flexible rockfall barriers subject to punching and areal loads.* Technical Note No. TN 4/2014. Geotechnical Engineering Office, Civil Engineering and Development Department, The HKSAR Government.

Kwan, J.S.H., and Sun, H.W. 2006. "An improved landslide mobility model." Canadian Geotechnical Journal 43(5): 531-539. https://doi.org/10.1139/t06-010.

Law, R.P.H., and Ko, F.W.Y. 2018. *Validation of geotechnical computer program "2d-DMM (Version 2.0)".* GEO Report No. 332. Geotechnical Engineering Office, Civil Engineering and Development Department, The HKSAR Government.

Li, X., and Zhao, J. 2018. "A unified CFD-DEM approach for modeling of debris flow impacts on flexible barriers." *International Journal for Numerical and Analytical Methods in Geomechanics* 42(14): 1643–1670. https://doi.org/10.1002/nag.2806.

Ma, D. and Liu, C. 2015. "Contact law and coefficient of restitution in elastoplastic spheres." *Journal of Applied Mechanics* 82(12): 121006. https://doi.org/10.1115/1.4031483.

Wang, H., Yin, X., Hao, H., Chen, W. and Yu, B. 2020. "The correlation of theoretical contact models for normal elastic-plastic impacts." *Int. J. Solids Struct.* 182:15–33. https://doi.org/10.1016/j.ijsolstr.2019.07.018.

Yigit, A.S., Christoforou, A.P., and Majeed, M.A. 2011. "A nonlinear visco-elastoplastic impact model and the coefficient of restitution." *Nonlinear Dynamics 66*(4): 509–521. https://doi.org/10.1007/s11071-010-9929-6.